Lysosomal Membrane Cholesterol Dynamics†

Jonathan K. Schoer,‡ Adalberto M. Gallegos,‡ Avery L. McIntosh,‡ Olga Starodub,§ Ann B. Kier,§ Jeffrey T. Billheimer,|| and Friedhelm Schroeder*,‡

Department of Physiology and Pharmacology and Department of Pathobiology, Texas A&M University, TVMC, College Station, Texas 77843-4466, and Cardiovascular Department, DuPont Merck Pharmaceutical Company, Experimental Station 400-3231, Wilmington, Delaware 19898-0400

Received November 22, 1999; Revised Manuscript Received March 23, 2000

ABSTRACT: Although the majority of exogenous cholesterol and cholesterol ester enters the cell by LDL-receptor-mediated endocytosis and the lysosomal pathway, the assumption that cholesterol transfers out of the lysosome by rapid (minutes), spontaneous diffusion has heretofore not been tested. As shown herein, lysosomal membranes were unique among known organellar membranes in terms of cholesterol content, cholesterol dynamics, and response to cholesterol-mobilizing proteins. First, the lysosomal membrane cholesterol:phospholipid molar ratio, 0.38, was intermediate between those of the plasma membrane and other organellar membranes. Second, a fluorescence sterol exchange assay showed that the initial rate of spontaneous sterol transfer out of lysosomes and purified lysosomal membranes was extremely slow, $t_{1/2} > 4$ days. This was >100-fold longer than that reported in intact cells (2 min) and 40−60-fold longer than from any other known intracellular membrane. Third, when probed with several cholesterol-binding proteins, the initial rate of sterol transfer was maximally increased nearly 80-fold and the organization of cholesterol in the lysosomal membrane was rapidly altered. Nearly half of the essentially nonexchangeable sterol in the lysosomal membrane was converted to rapidly ($t_{1/2} = 6$ min; fraction = 0.06) and slowly ($t_{1/2} = 154$ min; fraction = 0.36) exchangeable sterol domains/pools. In summary, the data revealed that spontaneous cholesterol transfer out of the lysosome and lysosomal membrane was extremely slow, inconsistent with rapid spontaneous diffusion across the lysosomal membrane. In contrast, the very slow spontaneous transfer of sterol out of the lysosome and lysosomal membrane was consistent with cholesterol leaving the lysosome earlier in the endocytic process and/or with cholesterol transfer out of the lysosome being mediated by additional process(es) extrinsic to the lysosome and lysosomal membrane.

Mammalian cells take up exogenous cholesterol and cholesterol ester by multiple pathways (reviewed in refs *1*−*4*). The majority of exogenous cholesterol and cholesterol ester enters the cell via LDL-receptor endocytosis (reviewed in ref *1*). Briefly, in this pathway the LDL binds to a receptor in a cell surface microdomain, the clathrin-coated pit. LDL bound to clathrin-coated pits is then endocytosed to form clathrin-coated vesicles which move toward the lysosome. Prior to fusing with lysosomes, the vesicles apparently shed most of their LDL unesterified cholesterol into the cytoplasm as small vesicles (reviewed in refs *5*−*7*). The LDL cholesterol ester, representing the majority of LDL sterol taken up, then enters the lysosomal pathway by fusion of the remnant vesicle with the lysosome. LDL cholesterol esters are rapidly hydrolyzed within the lysosomal matrix, followed by transfer of cholesterol out of the lysosome to other organelles by as yet unresolved process(es).

The time frame of LDL-receptor-mediated uptake of cholesterol ester in intact cells is not limited by the rate of sterol transfer out of the lysosomal compartment. The half-time for the overall process whereby LDL cholesterol ester enters the cell, is hydrolyzed to unesterified cholesterol within the lysosome, is transferred to the lysosomal membrane, is released from the lysosome, and thereafter appears at the plasma membrane is 42−60 min (*8*−*10*). The step involving transfer of cholesterol from the lysosomal matrix into, across, and out of the lysosomal membrane followed by appearance of the released cholesterol at the cell surface takes place within 2 min in intact cells (*10*). This very rapid transfer of cholesterol out of the lysosome has led to the assumption that sterol transfer out of the lysosome into the cell cytoplasm occurs by spontaneous, passive diffusion (*11*). However, this assumption has yet to be proven.

Despite the importance of the lysosome in cellular LDL-receptor-mediated uptake of cholesterol and cholesterol esters, there is paucity of data on the cholesterol dynamics in isolated lysosomes and a complete absence of data on the isolated lysosomal membrane (*12*). The lipid composition has been reported only for lysosomes obtained from animals treated with the detergent Triton or large indigestible particles of dextran (*13*−*15*). While this yielded a cholesterol:phospholipid ratio of 0.4−0.5 for dextranosomes and tritosomes, these altered lysosomes contained LDL cholesterol,

† This work was supported in part by a grant from the USPHS National Institutes of Health (GM31651).

* To whom correspondence should be addressed. TEL: 979-862-1433. FAX: 979-862-4929. E-MAIL: fschroeder@cvm.tamu.edu.

‡ Department of Physiology and Pharmacology, Texas A&M University.

§ Department of Pathobiology, Texas A&M University.

|| Cardiovascular Department, DuPont Merck Pharmaceutical Co.

10.1021/bi992686h CCC: $19.00
Published on Web 06/08/2000

cholesterol ester, and triglyceride as well as other constituents (the detergent Triton or dextran) in the lysosomal matrix (*12*). Since the above cholesterol:phospholipid ratio may therefore not accurately reflect that of the lysosomal membrane, to date essentially nothing is known about the lysosomal membrane cholesterol and its dynamics.

The focus of the work presented herein was to test the hypothesis that the transfer of sterol out of the lysosome and lysosomal membrane occurs via rapid, spontaneous diffusion. Lysosomes and lysosomal plasma membranes were isolated from cultured L-cell fibroblasts, and their cholesterol dynamics were examined with a fluorescent sterol transfer assay. Several unique, new insights into lysosomal cholesterol dynamics were obtained: (i) The lipid content (especially cholesterol and cholesterol/phospholipid) of the lysosomal membrane did not resemble either that of the endocytosed plasma membrane or that of other intracellular membranes. (ii) The spontaneous transfer of cholesterol out of the lysosome and lysosomal membrane was extremely slow, a $t_{1/2}$ of many days. This key observation was not consistent with rapid, spontaneous diffusion of sterol out of the lysosome and lysosomal membrane. (iii) The intrinsic proteins present in the lysosome and lysosomal membrane did not alone mediate rapid transfer of cholesterol out of the lysosomal membrane. (iv) Lysosomal membrane cholesterol dynamics were not a fixed property, as previously reported for membranes such as erythrocytes (*16*). Instead, probing with cholesterol-binding proteins induced the formation of very rapidly exchangeable sterol domains (half-time < 6 min) in lysosomal membranes.

MATERIALS AND METHODS

Materials. Dehydroergosterol (DHE)[1] was synthesized and purified as described previously (*17, 18*) or purchased from Sigma Chemical Co. (St. Louis, MO) and used without additional purification. Cholesterol and ergosterol were purchased from Steraloids (Wilmington, NH) and used without additional purification. Stock DHE (5 mg/mL) and cholesterol (10 mg/mL) solutions were prepared in 95% EtOH containing 1 mol % butylated hydroxytoluene (BHT) and stored at −70 °C. Percoll was purchased from Sigma Chemical Co. Metrizamide was purchased from Accurate Chemical and Scientific Corp. (Westbury, NY). Other chemicals were of reagent-grade or better and used without purification.

Monoclonal antibodies to lysosomal-associated membrane protein (anti-LAMP-2) and plasma membrane Na^+K^+-ATPase (anti-Na^+K^+-ATPase) were purchased from the Developmental Studies Hybridoma Bank (University of Iowa, Iowa City, IA). A polyclonal antibody to 70 kDa mitochondrial heat shock protein (anti-HSP70) was obtained from Analytical BioReagents (Golden, CO). Polyclonal antibody to catalase (anti-catalase) was obtained from Biodesign International (Kennebunkport, ME). A polyclonal antibody to microsomal 78 kDa glucose regulated protein (anti-GRP-78) was purchased from StressGen (Victoria, BC, Canada). Human recombinant SCP-2 (13 kDa) and pro-SCP-2 (15 kDa) were isolated as previously described (*19*). Rat recombinant L-FABP and I-FABP were isolated as described earlier (*20, 21*). Polyclonal antibody to SCP-2 (anti-SCP-2) was purified from antisera obtained from female NZW rabbits as described (*22*). The antibody reacted positively with all SCP-2 gene products.

Cell Culture. Murine L-cells (L $aprt^-tk^-$ from Dr. David Chaplin, Washington University, St. Louis, MO) and L-cells transfected with the cDNA encoding the 15 kDa pro-SCP-2 or the 13 kDa SCP-2 (*23*) were cultured in Higuchi media supplemented with 10% serum (Sigma Chemical Co.), 0.5% PenStrep (Gibco BRL, Grand Island, NY), and the necessary quantities of dehydroergosterol (DHE) and cholesterol as previously described (*24, 25*) with the following modifications. First, cells were grown in 200 mm × 200 mm culture trays (Nalge-Nunc, Milwaukee, WI) for a total of 90 h. Second, after 72 h the medium was removed, the cells were washed with phosphate-buffered saline (PBS), 80 mL of serum-free medium was added, and the cells were cultured for an additional 18 h. Third, for the exchange assay, donor and acceptor lysosomes were isolated from cells grown in media containing 15 μg/mL DHE (donor) or 15 μg/mL cholesterol (acceptor). Fourth, for the exchange assay standard curve, the DHE concentration in the medium was varied from 0 to 30 μg/mL.

Lysosomal Membrane Isolation. All procedures were performed with ice-cold solvents and chilled equipment. All buffer solutions were prepared using deionized water. After 90 h of growth, the medium was removed, the cells were rinsed twice with PBS, and the cells were harvested in isotonic sucrose/TRIS/EDTA (0.25 M sucrose/10 mM TRIS-HCl/1 mM EDTA, pH 7.4), centrifuged for 10 min at 3000*g* with a JA25.5 fixed-angle rotor on an Avanti J25 Centrifuge (Beckman Inc., Fullerton, CA), resuspended in a known volume of isotonic sucrose/TRIS/EDTA, and counted. The cells were homogenized in a N_2 Bomb Cell Disrupter (Parr Instrument Co., Moline, IL) with ∼35 psi of N_2 for ∼12 min. The post-nuclear supernatant was collected following centrifugation at 3000*g* for 10 min with a JA25.5 fixed-angle rotor on an Avanti J25 Centrifuge (Beckman Inc.). The pellet was resuspended in isotonic sucrose/TRIS/EDTA and homogenized again, and the post-nuclear supernatant was collected after low-speed centrifugation and combined with the previous post-nuclear supernatant.

Intact lysosomes were isolated from the post-nuclear supernatant generally following the differential centrifugation procedure described by Storrie and Madsen (*26, 27*). The post-nuclear supernatant was placed on top of a discontinuous gradient composed of layers of 6% Percoll, 17% metrizamide, and 35% metrizamide each in sucrose/TRIS/EDTA. After centrifugation for 35 min at 70000*g* with an SW40Ti rotor and model XL90 ultracentrifuge (Beckman Instruments), the band of partially purified lysosomes at the interface of the 6% Percoll and 17% metrizamide layers was collected. Additionally, the band between the 17% and 35% metrizamide layers containing enriched mitochondria was collected. The partially purified lysosomes were combined with 80% metrizamide to make a 35% metrizamide solution. The resulting solution was placed in the bottom of a centrifuge tube and overlaid with solutions of 17% metrizamide, 5% metrizamide, and sucrose/TRIS/EDTA. The gradient was centrifuged for 35 min at 70000*g* with an

[1] Abbreviations: DHE, dehydroergosterol; PBS, phosphate-buffered saline; BHT, butylated hydroxytoluene; SCP-2, 13 kDa sterol carrier protein-2; pro-SCP-2, 15 kDa pro-sterol carrier protein-2; L-FABP, liver fatty acid binding protein; I-FABP, intestinal fatty acid binding protein.

SW40Ti rotor and model XL90 ultracentrifuge (Beckman Instruments), and the band containing the enriched lysosomes was collected at the interface of the 5% metrizamide and 17% metrizamide solutions.

Intact lysosomes were lysed for 30 min in a hypotonic solution containing 0.025 M sucrose/1 mM TRIS-HCl, pH 7.4, as described earlier (*28*). The lysosomal membranes were then sedimented by centrifugation for 60 min at 112000*g* with an SW28 rotor and model UL60 ultracentrifuge (Beckman Instruments). The supernatant (lysosomal matrix) was discarded. The pellet was rinsed once with buffer and then resuspended in a minimum volume of 10 mM PIPES solution, pH 7.4, containing 1 mM EDTA. Total lysosomal membrane protein was determined immediately after isolation using a modified Lowry assay (*25, 29*).

The relative purity of intact lysosomes and lysosomal membranes was monitored by three methods. First, specific membrane enzyme markers were used (*25, 26, 30*−*32*). Second, since trace-residual metrizamide may suppress the enzyme activity of some lysosomal markers (*26, 33, 34*), quantitative Western blotting was also performed with both the intact lysosomes and the lysosomal membrane fractions, essentially as previously described for other L-cell proteins (*35, 36*). Protein was quantitated by densitometry following Western blot image acquisition with a model IS-500 system composed of a single-chip charge couple device video camera and computer workstation (Alpha Innotech, San Leandro, CA). The images were analyzed (mean 8-bit gray scale) using NIH Image (written by W. Rasband and available by anonymous FTP from zippy.nimh.nih.gov) on a Power Macintosh workstation. Third, the purity of the lysosomal membranes was also monitored by lipid analysis (see below) to determine if trapped lipoproteins (containing cholesterol esters) were present in the lysosomal membrane fraction. However, HPLC analysis of lipid extracts of purified lysosomal membranes contained almost no detectable cholesterol ester.

Lipid Extraction and Quantification. Lipids from lysosomal membranes were extracted in *n*-hexane/2-propanol (3:2 v/v), evaporated to dryness, redissolved in $CHCl_3$, and added to preactivated silicic acid (Clarkson Chemical Co., Inc.) columns ~2.5 cm in length. Neutral lipids were eluted with 4 column volumes of 59:1 $CHCl_3$/MeOH as previously described (*37*). The phospholipids were then eluted with 4 column volumes of MeOH.

The neutral lipid fraction was evaporated to dryness under N_2, redissolved in *n*-hexane/2-propanol/acetic acid (98.7:1.2:0.1 v/v/v), and filtered through a 0.2 μm nylon filter (Rainin Instrument Co., Inc., Woburn, MA). The resulting solution was evaporated to dryness under N_2 and resuspended in 100 μL of *n*-hexane/2-propanol/acetic acid (99.03:0.9:0.07 v/v/v). Cholesterol and DHE were quantified by high-performance liquid chromatography (HPLC). Ergosterol served as an internal standard. The HPLC system consisted of a model 110A HPLC pump (Alltec, now Beckman Instruments), a Phenomenex (Torrance, CA) Luna 5 μm silica 2 column (250 × 4.6 mm), a Shimadzu (Kyoto, Japan) SPD-10 UV−visible spectrophotometer, and a data acquisition system composed of a UI-20 A−D converter interface and PeakNet software (Dionex Inc., Sunnyvale, CA) operating on a PC-compatible computer. The mobile phase was identical to the sample solvent and was degassed with He prior to and during use. Separation conditions were as follows: 0.6 mL/min flow rate, isocratic elution profile, 55 °C column temperature, and detection at 205 nm. The phospholipid fraction was used to quantify the total phospholipid as previously described (*37*). Briefly, the samples were placed in acid-washed tubes, diluted with deionized water, and digested for 1 h at 180 °C in the presence of perchloric acid. Ammonium molybdate and ascorbic acid were then added to the solution, which was then heated for 5 min in a boiling water bath. After cooling, the absorbance was recorded at 797 and 660 nm and the total phosphorus quantified.

Sterol Transfer between Membranes. Sterol transfer between isolated lysosomal membranes was monitored generally following a procedure as previously described by our laboratory for other biological and model membranes (*16, 24, 38*−*43*). Briefly, DHE, a fluorescent and close structural analogue of cholesterol, was used as a probe for studying lysosomal membrane cholesterol dynamics. Our laboratory previously showed that murine L-cell fibroblasts grown in media containing DHE are an excellent probe molecule for cholesterol: DHE readily substitutes for greater than 80% of membrane cholesterol; DHE colocalizes with cholesterol and other sterols in the membranes; DHE does not significantly change the composition of other lipid constituents; DHE does not alter membrane structural or functional properties (*16, 25, 42, 44*). In this method, the fluorescence polarization of DHE was recorded as a function of time. Because the DHE content of the donor membranes was initially high, the DHE polarization was low, due to self-quenching. As DHE was transferred between donor membranes (initially containing high DHE) and acceptor membranes (initially lacking DHE), the fluorescence polarization increased. A standard curve to relate the fluorescence polarization to the membrane concentration of DHE allowed calculation of the molar rate at which DHE was transferred between lysosomal membranes and also determined the presence of DHE in single or multiple kinetic sterol domains. The general procedure is described below:

Steady-state fluorescence measurements (intensity and polarization) were recorded with a modified SLM-4800 Spectrofluorometer (ISS Instruments, Inc., Urbana, IL) with photon-counting electronics. The instrument was configured in the T-format with the emission monochromator removed. A 300 W Xe arc lamp served as the excitation source, and the excitation wavelength was set to 324 nm with a monochromator (8 nm spectral slit width). To reduce photobleaching, samples were continuously stirred, neutral density filters were placed in the excitation light path, and 0.5 mm entrance and exit slits were used on the excitation monochromator. Artifacts due to inner filter effects and light scatter were minimized by monitoring the emission through KV-389 low-fluorescence cutoff filters (Schott Glass Technologies, Inc., Duryea, PA) and by keeping the absorbance of sample solutions at the excitation wavelength (324 nm) below 0.15. The contribution of residual light scatter to exchange data was corrected by subtracting the residual fluorescence anisotropy of both donor and acceptor membranes from all experimental data.

All fluorescence polarization experiments were conducted in filtered 10 mM PIPES buffer solution, pH 7.4, using a cuvette thermostated to 37 ± 0.3 °C. Samples contained 7 μg/mL total protein of donor lysosomal membranes. The

DHE fluorescence polarization was monitored for 10 min to ensure a stable signal and obtain an initial value for the fluorescence polarization. Enough acceptor lysosomal membranes were then added to the cuvette to generate a 10-fold excess (70 μg/mL final concentration of total protein) of the acceptor membranes. The DHE polarization was subsequently recorded during 20 s intervals for 4 h to monitor sterol transfer between membranes.

Consistent with previous results, addition of the proteins used herein (SCP-2, pro-SCP-2, L-FABP, I-FABP) to donor membranes (absence of acceptor membranes) did not alter the fluorescence polarization of DHE (*24*, *31*, *40*, *42*) because of the following: (i) The affinity of the membrane for sterol is much higher than that of SCP-2 such that at equilibrium only a small portion of sterol is bound to SCP-2 (reviewed in refs *45*, *46*). In contrast, sterol micelles have a much lower affinity for sterol than membranes, and in the presence of micellar sterols (dehydroergosterol, cholesterol, NBD-cholesterol), saturation binding of sterol to SCP-2 can be observed (*47*−*49*). (ii) Fluorescence polarization of dehydroergosterol bound to SCP-2 (*47*) is not higher than that of self-quenched dehydroergosterol in membranes (see Results and refs *24*, *31*, *40*, *42*).

Determination of Standard Curves for the Sterol Exchange Assay. Standard curves were constructed to convert the fluorescence polarization of DHE to the distribution of DHE in the lysosomal membranes basically as described earlier (*16*, *24*, *38*−*43*). Plots of polarization versus mole fraction of DHE (as a function of total membrane lipid) were constructed after measuring the fluorescence polarization and the DHE content of a series of lysosomal membranes isolated from L-cells cultured in media containing varying amounts of DHE (see above). According to Weber (*50*), such a relationship is described by the hyperbolic function in eq 1:

$$P = P_0C/(B + C) \quad (1)$$

where P is the measured fluorescence polarization of DHE at concentration C in the membranes, P_0 is the DHE polarization at its infinite dilution in the membranes, and B is a constant.

Because eq 1 describes the polarization−concentration relationship for DHE in donor membranes only and the measured polarization in the assay is the result of the combined polarization of DHE in both the donor and acceptor membranes, eq 1 was modified to incorporate the contribution of DHE in the acceptor membranes. The concentrations of DHE in the donor (X_d) and acceptor (X_a) membranes were written as

$$X_d = C_d/C_t \quad (2)$$

$$X_a = 1 - X_d = 1 - (C_d/C_t) \quad (3)$$

where C_t was the concentration of DHE at time $t = 0$ and C_d was the concentration of DHE in the donor membrane at any later time, t. Anisotropy (r) is an additive function while polarization is not. To combine the contribution of DHE in the donor and acceptor membranes to the total fluorescence polarization, polarization values were converted to anisotropy in eq 4:

$$r = 2P/(3 - P) \quad (4)$$

The calculated anisotropy of donor and acceptor membranes was then described by eq 5:

$$r = f_dr_d + f_ar_a \quad (5)$$

where f_a and f_d were the fractions of DHE in the donor and acceptor membranes and r_a and r_d were the fluorescence anisotropies of the donor and acceptor membranes.

By combining eqs 1−5, recalling that the exchange assay is performed with a 10-fold excess of acceptor membrane, and combining several terms, the anisotropy was described in terms independent of the mole fraction of DHE in the acceptor membranes (eq 6):

$$r = r_0\{X_d/(1 + DX_d)\} + r_0\{(1 - X_d)/(1 + (D/10)(1 - X_d))\} \quad (6)$$

where r_0 was the anisotropy of DHE at infinite membrane dilution. The constant D was related to r_0 and the constant B from eq 1 through eq 7:

$$D = ZB[1 + (r_0/2)] \quad (7)$$

where Z was the mole fraction of DHE in the total membrane lipid. The parameter Z was estimated by eq 8:

$$Z = (P_0 - P)/PB \quad (8)$$

where P_0 and B were from eq 1 and P was the fluorescence polarization of DHE in the donor membranes in the absence of acceptor membranes. The first and second terms in eq 5 were the contributions to the anisotropy by the donor and acceptor membranes, respectively. Fluorescence polarization was then calculated from the anisotropy by using eq 9:

$$P = 3r/(2 + r) \quad (9)$$

Standard curves relating the mole fraction of DHE in the donor membranes (X_d) to the measured fluorescence polarization were then calculated for various initial concentrations of DHE in the donor membranes. The fraction of DHE remaining in the donor lysosomes during an exchange assay was calculated by best fit of the data to a polynomial equation of the form:

$$P = \Sigma b_nX_d^n$$

For sterol exchange between lysosomal membranes, a polynomial with two terms yielded a fit with $r^2 = 0.9992$ (eq 10) where $y(0) = 0.2186$ and $b_2 = -0.0836$.

$$F(x) = y(0) + b_2X_d^2 \quad (10)$$

Calculation of the Initial Rate of Sterol Transfer. The initial rate of DHE exchange between lysosomal membranes was estimated from the first 10 min of exchange data by using a standard curve essentially as previously described (*24*). Equation 10 describes the exchange between lysosomal membranes. Taking the time derivative of eq 10 yields

$$(dP/dt) = 2b_2X_d(dX_d/dt) \quad (11)$$

as $t \rightarrow 0$, $X_d \rightarrow 1$ (See Results, Figure 6). Using this relationship and rearranging eq 11 yield

$$1/2b_2(dP/dt)|_{t\to 0} = (dX_d/dt)|_{t\to 0} \quad (12)$$

To obtain the molar transfer rate of DHE (d[DHE]/dt), not dX_d/dt, dX_d/dt, was transformed into d[DHE]/dt by factoring in the initial donor membrane concentration (3.5 μg of protein/mL), the total sterol concentration in the lysosomal membranes (153 pmol/μg of protein), the mole percent of DHE in the donor membranes (7.5%), and the value of b_2 (−0.0836). Combining this information with eq 12 yielded eq 13:

$$(d[DHE]/dt)|_{t\to 0} = -0.241(dP/dt)|_{t\to 0} \quad (13)$$

The initial rate of DHE transfer was directly estimated by substituting the initial measured rate of fluorescence polarization change for $(dP/dt)|_{t\to 0}$.

Immunocytochemistry. Colocalization of SCP-2 with catalase was performed as described earlier (*22*). For colocalizing SCP-2 and LAMP2, antibodies to SCP-2 and to LAMP2 were diluted 1:20 and 1:50, respectively. Secondary antibodies were Texas Red-conjugated goat anti-rabbit IgG (1:100) for identifying SCP-2 and FITC-conjugated goat anti-mouse polyvalent IgG (1:200) for identifying lysosomal membrane protein LAMP2. L-cell fibroblasts were transfected with the cDNA encoding the 15 kDa pro-SCP-2 (*23*). In these cells as in normal tissues, pro-SCP-2 was posttranslationally converted to mature 13.2 kDa SCP-2 (*23*). The cells were fixed and permeabilized using 3.7% formaldehyde and 1.4% methanol in phosphate-buffered saline (PBS), pH 7.2, for 15 min, and 1% Triton X-100 in PBS for 5 min. The cells were then washed extensively (5× in 30 min) with 0.1% Tween 20 in PBS. Residual autofluorescence was quenched with 100 mM NH_4Cl in PBS; 2% ovalbumin in phosphate-buffered saline was used to block nonspecific reactivity. All incubations with antibodies (primary antibodies diluted in 1% ovalbumin in buffer; secondary antibodies diluted in buffer only) were performed for 30 min at 37 °C in a humidified chamber followed by subsequent extensive washing. Coverglasses were mounted on slides with anti-fade medium.

Laser Scanning Confocal Microscopy. Laser scanning confocal microscopy was performed with an MRC-1024 Laser Scanning Confocal Microscopy system equipped with a 15 mW Kr−Ar laser (Bio-Rad Inc., Hercules, CA). FITC was excited using the 488 nm laser line and emission detected through an OG515 long-pass filter. Texas Red was excited with the 568 nm laser line, and emission was monitored through a 680/32 band-pass filter. Cells were visualized with an Axiovert 135 inverted microscope, fitted with a 63×, 1.4 N.A. oil immersion lens (Zeiss Inc., New York, NY). Image acquisition, processing, and editing for printing were with Laser-Sharp (Bio-Rad Inc.), Meta Morph (Universal Imaging Corp., West Chester, PA), Photoshop (Adobe Systems Corp., Seattle, WA), and Claris Draw (Claris Corp./Filemaker Inc., Santa Clara, CA) software.

RESULTS

Purification of Lysosomes and Lysosomal Membranes. Cholesterol dynamics have heretofore not been reported for lysosomes or lysosomal membranes. Therefore, lysosomes were isolated from L-cell fibroblasts as described under Materials and Methods. Western blots of purified lysosomes show high levels of LAMP2 (Figure 1A, lane 3), a protein specific to lysosomal membranes, as compared to cell homogenate (Figure 1A, lane 2). In contrast, the peroxisomal marker catalase (Figure 1B, lane 3) and the mitochondrial marker heat shock protein 70 (Figure 1C, lane 3) were barely detectable in the lysosomes. The endoplasmic reticulum marker, 78 kDa glucose-regulated protein (Figure 1D, lane 3), was significantly reduced as compared to crude homogenate (Figure 1D, lane 2). Finally, the plasma membrane Na^+K^+-ATPase (Figure 1E, lane 3) markers also appeared reduced in lysosomes.

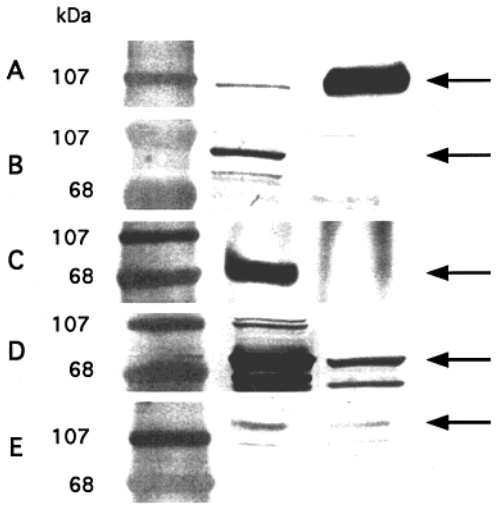

FIGURE 1: Western blotting of purified intact lysosomes. Western blots of purified lysosomes and crude homogenate were performed as described under Materials and Methods. Panel A, anti-LAMP2 (lysosomal membrane marker); panel B, anti-catalase (peroxisomal marker); panel C, anti-heat shock protein 70 (mitochondrial marker); panel D, anti-78 kDa glucose regulated protein (endoplasmic reticulum marker); panel E, anti-Na^+K^+-ATPase (plasma membrane marker).

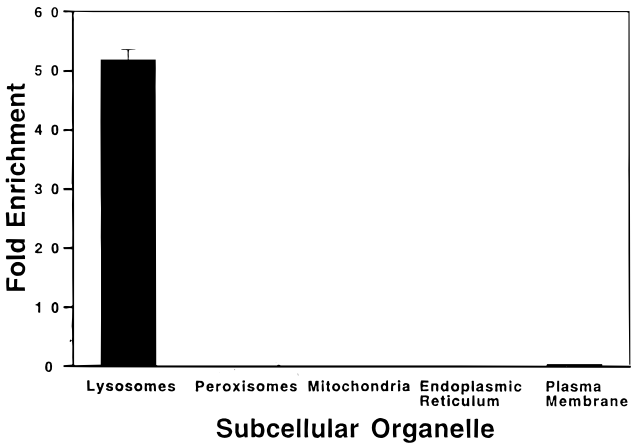

FIGURE 2: Fold enrichment of lysosomal fraction relative to cell homogenate. The results are based on Western blot analysis of the membrane marker proteins listed in Figure 1. Values represent the mean ± SD, $n = 3-5$.

Quantitative analysis of Western blots from three to five lysosome preparations was performed as described under Materials and Methods. The quantitative analysis demonstrated that the L-cell lysosome preparation was purified 52-fold with respect to LAMP2 as compared to cell homogenate (Figure 2). Concomitantly, markers for other organelles were dramatically reduced in the lysosomal preparation as compared to cell homogenate: peroxisomal catalase was decreased 42-fold; mitochondrial heat shock protein 70 was

reduced 29-fold; 78 kDa glucose-regulated protein was reduced 5-fold; Na^+K^+-ATPase was reduced 3−4-fold. The presence of some plasma membrane marker (Na^+K^+-ATPase) and endoplasmic reticulum marker (78 kDa glucose-regulated protein) in the lysosome preparation was expected due to continual recycling of endocytosed plasma membrane into the lysosomal compartment (*14*) and to autophagy of intracellular organelles (*51*), respectively. Our laboratory previously demonstrated that cell surface membrane cycling is especially rapid in L-cells, with the equivalent of the entire surface membrane being endocytosed every 2.1 h (*52*). Finally, lysosomal membranes isolated after osmotic lysis were purified an additional 2-fold (not shown). In summary, the results indicated that the lysosomal fraction and lysosomal membranes isolated from L-cells were highly enriched as compared to cell homogenate and decreased in markers for most other intracellular organelles.

Lysosomal Membrane Lipid Content. Although the lipid content has been determined for lysosomal derivatives, tritosomes and dextranosomes, these phagolysosomes contained endocytosed lipoproteins as well as Triton detergent or dextran (*12*−*15*). Since the actual cholesterol and phospholipid contents of the lysosomal membrane are not known, lipids were extracted from lysosomal membranes isolated from L-cell fibroblasts. The lysosomal membrane content of cholesterol and phospholipid was 46.0 ± 14.3 and 320.0 ± 21.8 μg/mg of membrane protein, respectively. Thus, the lysosomal membrane cholesterol:phospholipid ratio was 0.14 ± 0.01 (mg/mg) or 0.38 ± 0.03 (mol/mol). Cholesterol esters, indicative of lipoprotein contaminants in the purified lysosomal membranes, were not detected.

Effect of Increasing Dehydroergosterol Content on Dehydroergosterol Fluorescence Polarization in L-cell Fibroblast Lysosomal Membranes. To determine molecular sterol transfer by the fluorescent dehydroergosterol exchange assay, it was necessary to incorporate varying amounts of dehydroergosterol into lysosomal membranes. Membranes containing high quantities of dehydroergosterol are expected to exhibit concentration-dependent self-quenching, essential to the assay (*24*, *39*). Therefore, L-cells were cultured in the presence of increasing dehydroergosterol (0−30 μg/mL) in the medium as described under Materials and Methods. The lysosomal membranes were then isolated and separated into two aliquots: (i) One aliquot was used for determination of fluorescence polarization. Because polarization is calculated from a ratio of fluorescence intensities, it provided a more stable signal than the absolute fluorescence intensity, especially since it was necessary to measure sterol exchange over a period of hours. (ii) A second aliquot was used for determination of dehydroergosterol content. The lysosomal lipids were extracted, sterol content was determined, and the relative proportions of dehydroergosterol and cholesterol were determined by HPLC.

The data showed that dehydroergosterol was readily incorporated into L-cell lysosomal membranes (Figure 3). It should be noted, however, that supplementation of the L-cell growth medium with dehydroergosterol (0−30 μg/mL) did not significantly alter the sterol:phospholipid ratio in the lysosomal membranes, which remained constant near 0.14 ± 0.01 mg of sterol/mg of phospholipid. At low dehydroergosterol content, i.e., high ratio of 1/[100(DHE)/(total lipid)], the dehydroergosterol fluorescence polarization

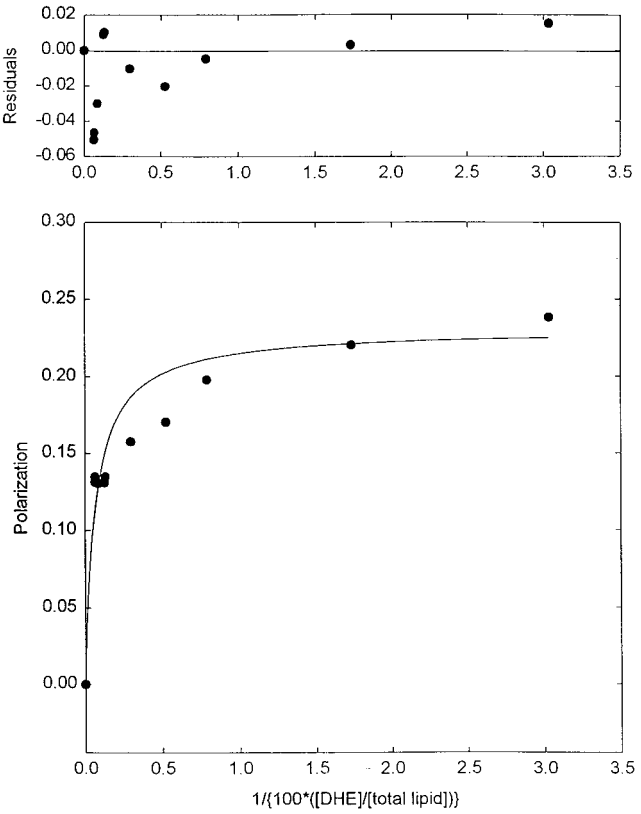

FIGURE 3: Polarization−concentration curves for lysosomal membranes. The concentration of DHE in membranes was determined as described under Materials and Methods. Fluorescence polarization was measured in the T-format using the blank subtraction mode. The blank consisted of the same concentration of lysosomal membranes that did not contain DHE.

was maximal near 0.23 (Figure 3). However, with increasing dehydroergosterol content, the dehydroergosterol fluorescence polarization in the lysosomal membranes decreased. This concentration-dependent decrease in dehydroergosterol polarization was consistent with Weber's theory of concentration-dependent fluorescence polarization (*50*). The solid line in Figure 3 (bottom panel) was the best fit of the experimental data to eq 1 with parameters $P_0 = 0.2317$, $B = 0.1144$, and $r^2 = 0.93$. P_0 represents the dehydroergosterol fluorescence polarization at its infinite dilution, i.e., in the absence of self-quenching. The residuals in Figure 3 (top panel) were randomly scattered except at very high dehydroergosterol concentrations, at which dehydroergosterol concentration was maximally quenched and, as expected, there was no further decrease in polarization.

Dehydroergosterol Fluorescence Polarization in L-cell Fibroblast Lysosomal Membranes: Construction of the Standard Curve. Although changes in dehydroergosterol polarization qualitatively show sterol transfer, they do not quantitatively show molecular sterol transfer. However, the latter can be obtained after construction of a standard curve for the exchange of dehydroergosterol between lysosomal membranes (see Materials and Methods). The standard curve for the sterol exchanges involving the lysosomal membrane donor−lysosomal membrane acceptor pair is shown in Figure 4. Initially, when the dehydroergosterol was self-quenched in the donor membrane, the polarization was low, near 0.135 (Figure 4). As the exchange progressed (decreasing mole fraction of dehydroergosterol in the donor lysosomal mem-

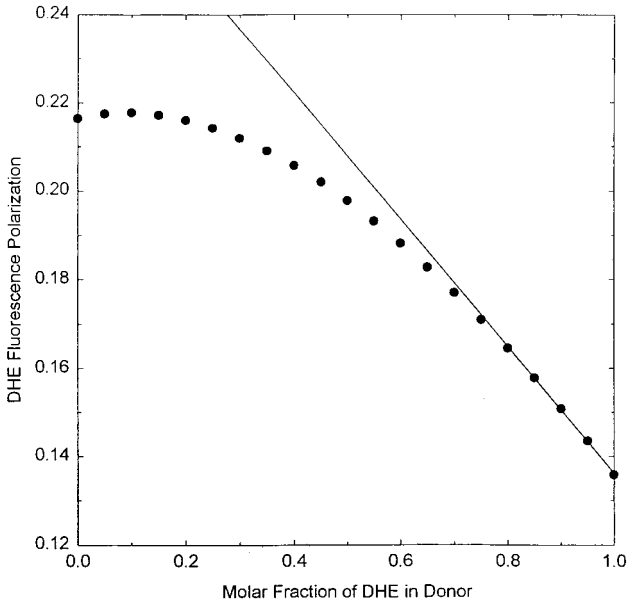

FIGURE 4: Standard curve for sterol exchange between lysosomal membranes in which the initial mole percent of DHE in the donor membranes was 7.5%. Standard curves were calculated using eq 6 (see Materials and Methods).

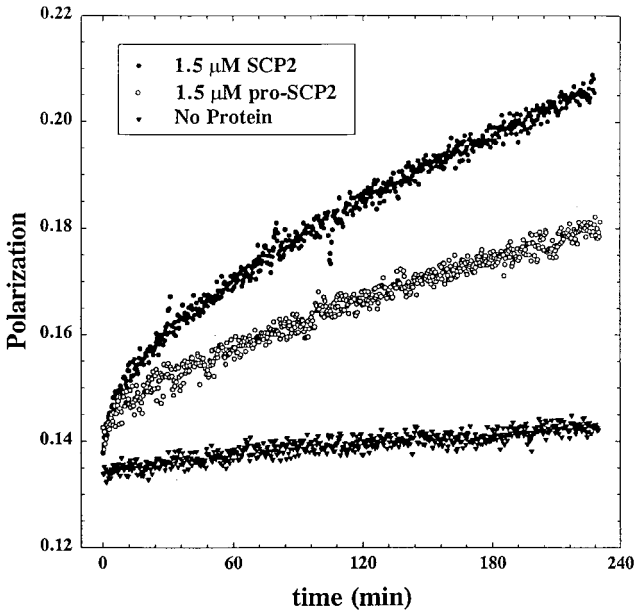

FIGURE 5: Effect of SCP-2 and pro-SCP-2 on sterol exchange between lysosomal membranes. The curves show the change in fluorescence polarization as a function of time after addition of a 10-fold excess of acceptor (DHE-poor) membranes to donor (DHE-rich) membranes. In the presence of 1.5 μM SCP-2 or pro-SCP-2, the exchange rate during the first 10 min was very fast and nearly linear (see Table 1).

brane), the dehydroergosterol polarization increased. The straight line shown in Figure 4 was a linear fit of the fluorescence polarization for mole fraction of dehydroergosterol (X_d) from 1.0 to 0.8 with an r^2 value of 0.9999. From this curve, it was apparent that the initial change in fluorescence polarization was directly proportional to the change in mole fraction of dehydroergosterol. As a result, it was possible to obtain the initial rate of molecular dehydroergosterol exchange between donor and acceptor membranes (without having to separate the donor and acceptor membranes) simply by comparison of polarization values to the standard curve.

Spontaneous Transfer of Sterol from Purified Lysosomal Membranes. The spontaneous exchange of sterol between lysosomal membrane donors and acceptors is depicted in Figure 5. In the absence of lysosomal membrane acceptors, dehydroergosterol polarization in lysosomal membrane donors did not significantly change over the time period examined (not shown). Addition of a 10-fold excess of acceptor lysosomal membranes elicited only a slow spontaneous sterol exchange from lysosomal membranes (Figure 5, bottom curve). The half-time for this spontaneous sterol transfer from the lysosomal membrane was estimated to be >4 days. The initial rate of spontaneous molecular sterol exchange between lysosomal membranes, determined using the above standard curve as described under Materials and Methods, was only 0.010 ± 0.002 pmol/min (Table 1). Comparison to results with other organelle membranes further confirmed that this rate was extremely slow: 63-fold slower than for plasma membranes, 41-fold slower than for microsomal membranes, 60-fold slower than for mitochondrial membranes (Table 1). In summary, the spontaneous transfer of sterol out of the lysosomal membrane was very slow. This observation was not consistent with rapid, spontaneous diffusion of cholesterol out of the lysosomal membrane.

Spontaneous Transfer of Sterol from Whole Lysosomes. The slow spontaneous sterol exchange from isolated lysosomal membranes detailed in the preceding section was not an artifact of the hypotonic lysis procedure used for isolating the lysosomal membranes. As shown in Figure 6, spontaneous sterol exchange from whole lysosomes was just as slow as from the isolated lysosomal membranes. Thus, both the extremely long half-time and the very slow initial rate of spontaneous sterol transfer from lysosomal membranes suggest that spontaneous diffusion of sterol out of the lysosomal membrane was unlikely to account for the relatively rapid (2 min) cholesterol efflux from this organelle noted in intact cells (*10*). Consequently, these data also did not support the assumption that cholesterol moved out of the lysosome by rapid, spontaneous diffusion.

Probing Lysosomal Membrane Cholesterol Dynamics. Prior to fusion with lysosomes, the clathrin-coated pits apparently shed vesicles as a mechanism for removal of unesterified cholesterol and for vesicle membrane remodeling (reviewed in ref *7*). Cells contain numerous proteins that bind cholesterol and accelerate intermembrane cholesterol transport in vitro and in transfected cells overexpressing the protein (reviewed in refs *4, 48, 53*). Therefore, such proteins were used as probe molecules to determine whether the very slow dynamics of cholesterol out of lysosomes and lysosomal membranes are a fixed property or whether cholesterol-binding proteins can induce transfer of cholesterol therefrom.

To be useful probes of sterol dynamics in lysosomal membranes determined by the fluorescent sterol transfer assay, the sterol-binding proteins must not themselves change the fluorescence polarization (*24, 31, 40, 42*). None of the proteins tested herein (SCP-2, pro-SCP-2, L-FABP, I-FABP) changed the fluorescence polarization of DHE in the absence of acceptor membranes (data not shown). The lack of change upon addition of these proteins to donor lysosomal membranes (in the absence of acceptor membranes) was due to several factors: First, these proteins enhance intermembrane

Table 1: Molar Sterol Transfer between Donor and Acceptor Membranes[a]

	initial rate of sterol transfer (pmol min^{-1})				
donor−acceptor	no protein	SCP-2	pro-SCP-2	L-FABP	I-FABP
LYSO−LYSO	0.010 ± 0.002 [1]	0.50 ± .08[c] (49)	0.18 ± 0.07[c] (18)	0.006 ± 0.002 (0.6)	0.006 ± 0.003 (0.6)
PM−PM[b]	0.65 ± 0.04 [63]	4.14 ± 0.64[c] (6.4)	−	0.97 ± 0.13[c] (1.5)	−
MICRO−MICRO[b]	0.42 ± 0.06 [41]	0.92 ± 0.18[d] (2.2)	−	0.28 ± 0.09 (0.7)	−
MITO−MITO[b]	0.62 ± 0.13 [60]	1.4 ± 0.08[d] (2.3)	−	0.53 ± 0.05 (0.9)	−

[a] Values represent the mean ± SD ($n = 4-9$). Values in parentheses are the fold enhancement caused by adding 1.5 μM protein relative to no protein. Values in square brackets are initial transfer rates in the absence of protein normalized to sterol transfer between lysosomal membranes. [b] Values obtained from (*24*). LYSO−LYSO, PM−PM, MICRO−MICRO, and MITO−MITO refer to exchange between lysosomal membranes, plasma membranes, microsomal membranes, and mitochondrial membranes, respectively. [c] $p < 0.01$ compared with no protein. [d] $p < 0.05$ compared with no protein.

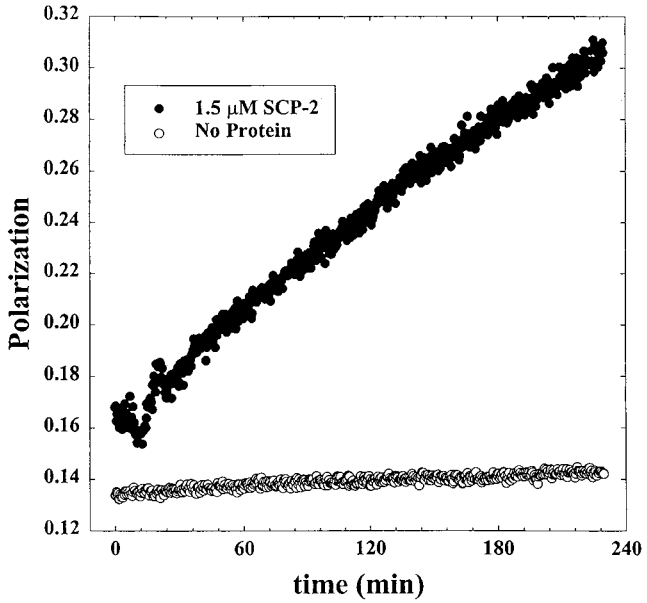

FIGURE 6: Sterol exchange between lysosomes. The curves show the change in fluorescence polarization as a function of time after addition of a 10-fold excess of acceptor (DHE-poor) to donor (DHE-rich) lysosomes in the absence (bottom curve) or presence (top curve) of 1.5 μM SCP-2.

cholesterol transfer by interacting with membranes (*54*−*59*). Second, although these proteins bind micellar cholesterol and dehydroergosterol (*47*, *48*, *60*−*62*), the affinity of membranes for sterol is sufficiently high that a soluble complex of the sterol-binding protein with cholesterol or dehydroergosterol is present only in very low amounts (reviewed in refs *45*, *46*, *63*, *6*). Third, the fluorescence polarization of dehydroergosterol bound to these proteins is not higher than that of self-quenched dehydroergosterol in membranes (*24*, *31*, *40*, *42*). Consequently, there was no increase in dehydroergosterol polarization upon sterol-binding protein addition to donor membranes (no acceptor membranes present).

Three classes of lipid-binding/transfer proteins were chosen as probes for lysosomal cholesterol dynamics (reviewed in ref *4*): (i) lipid transfer proteins that bind sterol and enhance sterol transfer between almost all membranes tested (sterol carrier protein-2, SCP-2; pro-sterol carrier protein-2, pro-SCP-2); (ii) lipid transfer protein that binds sterol and enhances sterol transfer only between select membranes (liver fatty acid binding protein, L-FABP); (iii) lipid transfer protein that neither binds nor enhances intermembrane sterol transport (intestinal fatty acid binding protein, I-FABP).

Probing Lysosomal Membrane Cholesterol Dynamics: Cholesterol-Binding Proteins with Broad Specificity in Enhancing Cholesterol Transfer. SCP-2 and pro-SCP-2 induced rapid sterol transfer between lysosomal membranes. In the presence of a 10-fold excess of lysosomal acceptor membranes and either SCP-2 (Figure 5, top curve) or pro-SCP-2 (Figure 5, middle curve), the dehydroergosterol polarization increased linearly for a period of 10−15 min. Addition of SCP-2 or pro-SCP-2 accelerated the polarization change for dehydroergosterol in the following order: SCP-2 > pro-SCP-2 ≫ spontaneous. By use of the appropriate standard curves as described under Materials and Methods, the initial rates of SCP-2- and pro-SCP-2-mediated dehydroergosterol polarization change were converted to initial rates of molecular sterol transfer (Table 1). Thus, SCP-2 and pro-SCP-2 increased the initial rate of molecular sterol transfer from lysosomal donor membranes by nearly 2 orders of magnitude: 49-fold and 18-fold, respectively.

The effects of SCP-2 on lysosomal membrane sterol transfer were observed over a wide concentration range (Figure 7A, 0.1−2.5 μM) and a wide range of SCP-2:membrane protein ratios (Figure 7B, 0.01−0.50 μg/μg). SCP-2 stimulation of the initial rates of molecular sterol transfer from lysosomal membranes was saturable as a function of SCP-2 concentration (Figure 7A). A Lineweaver−Burke plot of these data ($r^2 = 0.9984$) showed a K_m for SCP-2 of 1.0 μM and a limiting initial rate of sterol transfer induced by SCP-2 of 0.79 pmol/min, nearly 80-fold higher than spontaneous sterol transfer from lysosomal membranes.

Increasing the pro-SCP-2 showed typical saturation curves of the initial rates of molecular sterol transfer from lysosomal membranes (Figure 7). Although similar to the effects of SCP-2, pro-SCP-2 stimulated lysosomal membrane sterol transfer about 3-fold less over the same concentration range (Figure 7A, 0.1−2.5 μM pro-SCP-2) and range of transfer protein:membrane protein ratios (Figure 7B, 0.01−0.50 μg/μg). Pro-SCP-2 maximally increased the initial rate of molecular sterol transfer to 0.21 nmol min^{-1} mg^{-1} (Figure 7B, bottom curve). A Lineweaver−Burke plot of these data ($r^2 = 0.9937$) yielded a K_m of 0.67 μM and a limiting initial rate of pro-SCP-2-stimulated sterol transfer from the lysosomal membrane of 0.28 pmol/min, nearly 30-fold faster than

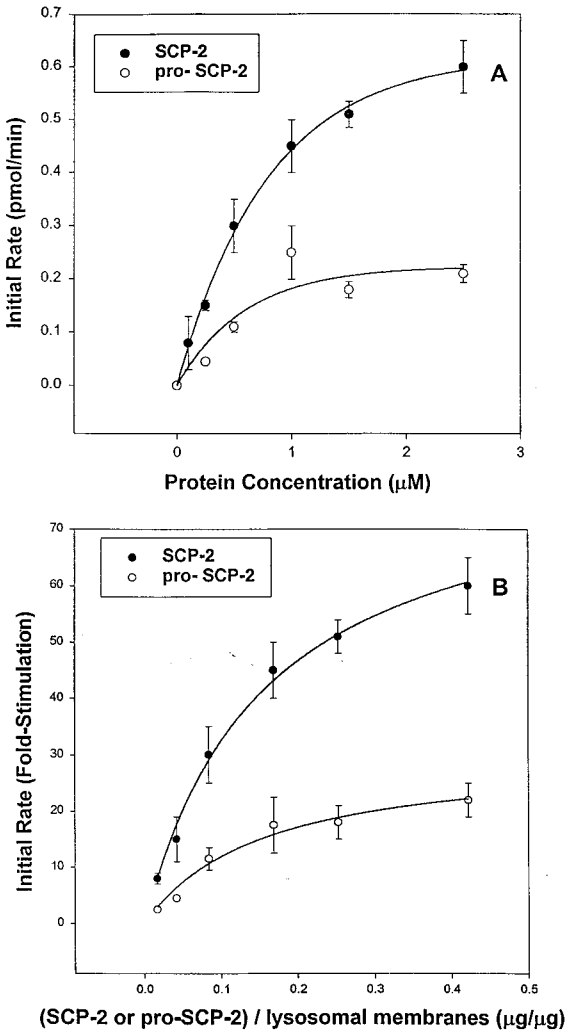

FIGURE 7: Dose dependence of SCP-2- and pro-SCP-2-mediated lysosomal membrane sterol exchange. The curves show the initial rate (pmol/min) of SCP-2 (solid circles) and pro-SCP-2 (open circles) mediated sterol transfer from lysosomal membranes as a function of protein (SCP-2 or pro-SCP-2) concentration (panel A) or ratio of protein (SCP-2 or pro-SCP-2) to lysosomal membrane protein. All conditions were as described in the legend of Figure 5, except that the SCP-2 or pro-SCP-2 concentration was varied from 0 to 3 μM.

spontaneous sterol transfer from the lysosomal membrane.

Finally, the SCP-2-mediated enhancement of sterol transfer from lysosomal membranes was not an artifact of the hypotonic lysis procedure used for isolating the lysosomal membranes. As shown in Figure 6, SCP-2 dramatically stimulated sterol transfer from whole lysosomes. Thus, the very slow initial rate of spontaneous sterol transfer from lysosomes and its enhancement by SCP-2 were consistent with observations on sterol transfer from isolated lysosomal membranes not being an artifact of the preparation.

Probing Lysosomal Membrane Cholesterol Dynamics: Proteins Which Exhibit Weak or No Specificity for Enhancing Intermembrane Cholesterol Transfer. Our laboratory previously showed that liver fatty acid binding protein L-FABP, but not intestinal fatty acid binding protein I-FABP, enhanced sterol transfer from plasma membranes (*24*, *65*). However, neither L-FABP (Figure 8a) nor I-FABP (Figure 8b) stimulated sterol transfer from lysosomal membranes. The

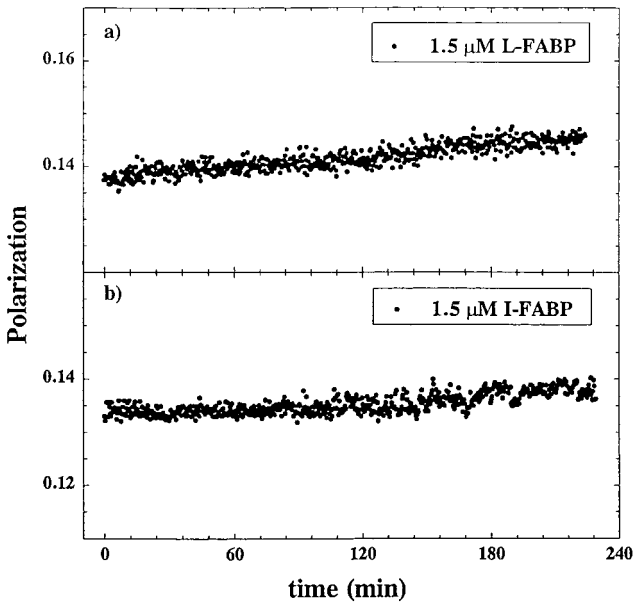

FIGURE 8: Effect of L-FABP and I-FABP on sterol exchange between lysosomal membranes. The curves show the change in fluorescence polarization as a function of time after addition of a 10-fold excess of acceptor (DHE-poor) membranes to donor (DHE-rich) membranes preincubated for 10 min with 1.5 μM L-FABP (panel a) or I-FABP (panel B). The shallow slope shows that neither L-FABP nor I-FABP stimulates the sterol transfer significantly.

initial rates of sterol transfer from lysosomal membranes in the presence of L-FABP and I-FABP were 0.006 ± 0.002 and 0.006 ± 0.003 pmol/min, respectively (Table 1). These initial rates of sterol transfer were not significantly different from spontaneous sterol transfer from lysosomal membranes, 0.010 ± 0.002 pmol/min. Thus, the effects of SCP-2 and pro-SCP-2 on lysosomal cholesterol transfer were specific.

Effect of Cholesterol-Binding Proteins on Lysosomal Membrane Exchange Dynamics: Role of Exchangeable and Nonexchangeable Domains. The spontaneous sterol exchange was so slow that it was impossible to fit it to multiple exponentials. Instead, the spontaneous transfer of sterol from lysosomal membranes best fit a single exponential with half-time >4 days, comprising 100% of the total sterol (Table 2). Therefore, this sterol pool/domain was designated as essentially nonexchangeable. As shown in the preceding sections, the lysosomal membrane sterol transfer dynamics were significantly altered by sterol-binding protein probes, including SCP-2 and pro-SCP-2. These proteins are known to bind to cholesterol-rich, acidic phospholipid-containing membranes, e.g., model membranes (*59*) and plasma membranes (*55*). It is thought that by doing so, the sterol-binding proteins induce formation of membrane microdomains through which cholesterol may transfer rapidly (reviewed in refs *4*, *48*, *53*). Therefore, this possibility was examined with lysosomal membranes.

SCP-2 and pro-SCP-2 induced the formation of rapidly exchangeable domains in lysosomal membranes. Both SCP-2- and pro-SCP-2-mediated sterol exchange curves did not fit a one-exponential equation, as indicated by an r^2 of 0.17. Instead, the same curves ($n = 4$) yielded an excellent fit to a two-exponential equation: $P = y_0 + ax + bx^2$, with an r^2 of 0.9999 and the resultant parameters $y_0 = 0.3403 \pm 0.0003$, $a = -0.0955 \pm 0.0015$, and $b = -0.0916 \pm 0.0015$.

Table 2: Kinetic Parameters of Spontaneous and Protein-Mediated Sterol Exchange between Lysosomal Donor and Acceptor Membranes[a]

	half-times (min)		kinetic domain fractions		
protein	$^1t_{1/2}$	$^2t_{1/2}$	f_1	f_2	f_3
none[b]	–	–	–	–	1.00 ± 0.00
SCP-2	5.5 ± 0.8	154 ± 12	0.059 ± 0.008	0.363 ± 0.012	0.578 ± 0.022
Pro-SCP-2	6.9 ± 1.1	193 ± 16	0.046 ± 0.007	0.337 ± 0.016	0.615 ± 0.026
L-FABP[c]	–	–	–	–	1.00 ± 0.00
I-FABP[c]	–	–	–	–	1.00 ± 0.00

[a] The values $^1t_{1/2}$ and $^2t_{1/2}$ are the half-times for the various kinetic sterol domains. The values f_1, f_2, and f_3 are the calculated fractions of rapidly exchangeable, slowly exchangeable, and very slowly (non)exchangeable sterol domains, respectively, in the lysosomal membranes. Values represent the mean ± SE, $n = 4-7$. [b] In the absence of protein, the spontaneous transfer of sterol between lysosomal membranes was best described by a single, very slowly or nonexchangeable domain. The exchange was so slow that the half-time could not be calculated reliably, but was estimated to be >4 days. [c] L-FABP and I-FABP did not stimulate sterol exchange from lysosomal membranes.

Addition of SCP-2 induced the formation of two exchangeable sterol domains in the lysosomal plasma membrane: a rapidly exchanging domain with $t_{1/2} = 5.5 \pm 0.8$ min and fraction 0.059 ± 0.008; a slowly exchangeable sterol domain with $t_{1/2} = 154 \pm 12$ min and fraction 0.363 ± 0.012 (Table 2). The induction of these exchangeable sterol domains by SCP-2 was at the expense of the nonexchangeable sterol domain whose fraction was reduced from 1.00 to 0.58 (Table 2). Similarly to SCP-2, pro-SCP-2 also induced formation of a rapidly exchangeable sterol pool and a slowly exchangeable sterol pool with half-times and fractions similar to those of SCP-2 (Table 2). In contrast, neither L-FABP nor I-FABP altered any of the half-times or kinetic domain fractions of cholesterol in lysosomal membranes. Thus, the data suggested that the effects of SCP-2 and pro-SCP-2 on lysosomal membrane cholesterol domains were specific and were mediated through alterations in lysosomal membrane domains.

Indirect Immunofluorescence Confocal Imaging of Transfected L-cells Expressing SCP-2. In addition to being useful as a probe for lysosomal membrane cholesterol dynamics in vitro, SCP-2's dramatic enhancement of sterol transfer from lysosomal membranes may also have functional significance. Although all SCP-2 gene products contain a C-terminal SKL peroxisomal targeting sequence, in order for SCP-2 to fulfill a functional role in potentially mediating cholesterol transfer from the lysosomes to other subcellular sites of intact L-cells SCP-2 must at least in part be localized with lysosomes and/or in the cytosolic space. This possibility was tested using L-cells transfected with the cDNA encoding the 15 kDa pro-SCP-2, encoded by the gene, or with the cDNA encoding the 13 kDa SCP-2 lacking the 20 amino acid presequence present in pro-SCP-2. The 15 kDa pro-SCP-2 is rapidly posttranslationally cleaved to the 13 kDa SCP-2 in almost all tissues and cells studied, including L-cells. Western blots of both transfectants revealed only the 13 kDa SCP-2 (reviewed in ref *48*).

The intracellular distribution of SCP-2 in the L-cells transfected with cDNA encoding the 15 kDa pro-SCP-2 was determined by immunofluorescence and confocal microscopy as described under Materials and Methods. In these experiments, the cells were simultaneously labeled with antibodies to catalase, a peroxisomal marker, and SCP-2. The two respective antibody markers were then visualized with different secondary antibody labels as indicated by pseudocolors: red for SCP-2 (Figure 9A) and green for catalase (Figure 9B). Both proteins were distributed in a punctate pattern. In addition, a portion of the SCP-2 immunolabeling pattern was diffuse in the cytosol. The degree of colocalization of SCP-2 and catalase was visualized by superposition of these simultaneously acquired confocal images of the same cell (Figure 9C). Colocalization was visualized as orange punctate areas. The fact that there were significant separate red (SCP-2) pixelated areas, as well as diffuse labeling, indicated lack of colocalization with catalase/peroxisomes in these areas. The degree of SCP-2 colocalization with peroxisomes was quantitatively expressed as a pixel scattergram (Figure 9D), confirming the presence of SCP-2 codistributed with catalase in peroxisomes (orange pixels along the diagonal of the scattergram). In addition, the scattergram showed diffuse as well as some distinct punctate extraperoxisomal labeling (red or green pixels away from the diagonal of the scattergram). Although it has been postulated that the site of 15 kDa pro-SCP-2 posttranslational cleavage lies within the peroxisome (*66*), these data were consistent with some extraperoxisomal, posttranslational cleavage of the 15 kDa pro-SCP-2 to yield the 13 kDa SCP-2.

In contrast to the 15 kDa pro-SCP-2, the 13 kDa SCP-2 contains only the C-terminal SKL peroxisomal targeting sequence. If the N-terminal 20 amino acid presequence of 15 kDa pro-SCP-2 diminished the targeting of the protein to peroxisomes (thereby giving rise to some extraperoxisomal 13 kDa SCP-2), then transfecting the cells with the cDNA encoding the 13 kDa SCP-2 should have resulted in almost exclusive targeting of the protein to peroxisomes. On the contrary, the intracellular distribution of SCP-2 in the L-cells transfected with cDNA encoding the 13 kDa SCP-2 showed very little peroxisomal colocalization as compared to that of cells transfected with cDNA encoding the 15 kDa pro-SCP-2. As expected, catalase was distributed in a punctate pattern typical of peroxisomes (Figure 10B). In contrast, the distribution of SCP-2 (Figure 10A) was both punctate and more weakly diffuse. The degree of colocalization of SCP-2 and catalase was visualized by superposition of these simultaneously acquired images of the same cell (Figure 10C). The paucity of orange punctate areas indicated only a minor degree of colocalization of the punctate catalase and punctate SCP-2. Instead, most of the SCP-2 was visualized as separate punctate and some diffuse red labeling. SCP-2 colocalization with peroxisomes was 5-fold lower (Figure 10D) than in pro-SCP-2 expressing cells (Figure 9D). Little SCP-2 codistributed with catalase in peroxisomes (orange pixels along the diagonal of the scattergram) and instead was primarily separate green and red pixels away from the diagonal of the scattergram. These data suggested that if the

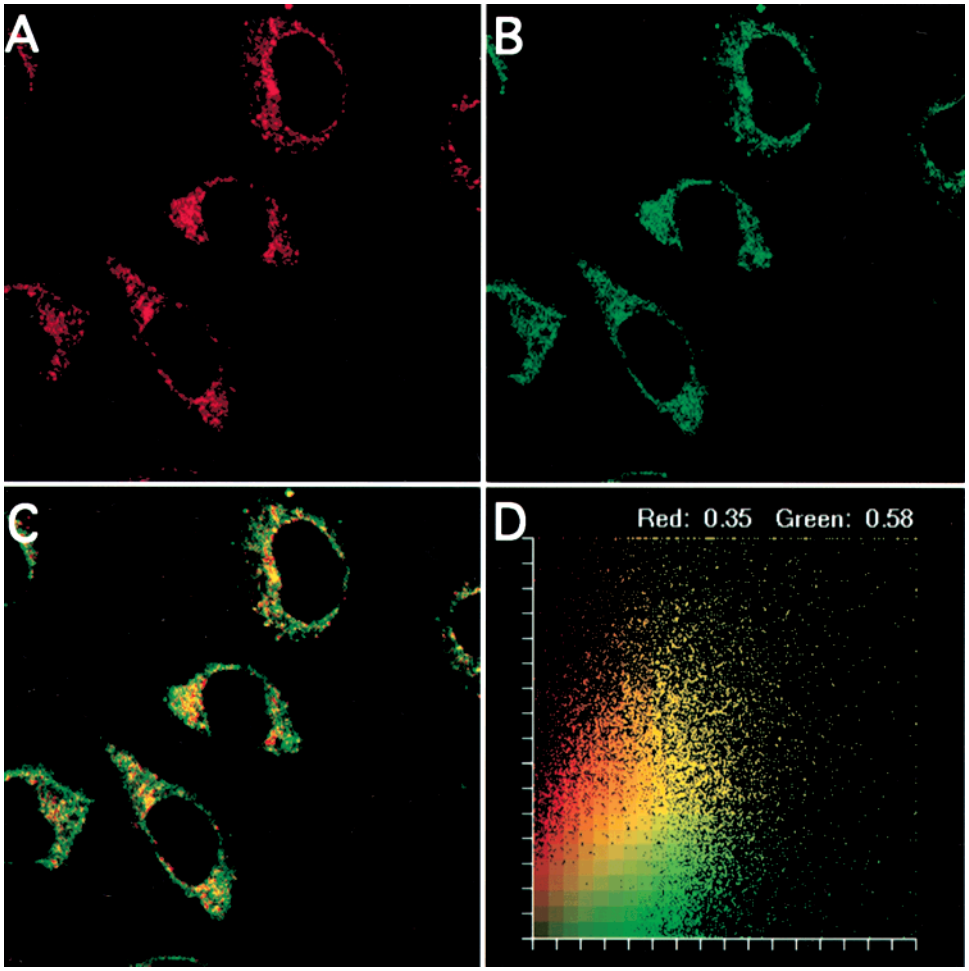

FIGURE 9: Confocal immunofluorescence imaging of L-cell fibroblasts transfected with the cDNA encoding 15 kDa pro-SCP-2: colocalization of SCP-2 with peroxisomal catalase. L-cells overexpressing 15 kDa pro-SCP_2 were simultaneously labeled with rabbit anti-SCP_2 and sheep anti-catalase followed by a Texas Red-conjugated IgG anti-rabbit secondary antibody (A, C) and FITC-conjugated IgG anti-sheep secondary antibody (B, C). Simultaneous double-label confocal images were acquired with a MRC 1024 laser scanning confocal microscopy system (Bio-Rad, Hercules, CA) with 63× objective and Axiovert 135 microscope (Zeiss Inc., New York, NY). Images are shown for SCP_2 (red, panel A) and catalase (green, panel B). Superposition of panels A and B yielded a merged image (panel C). Colocalized SCP_2 (red) with catalase (green) resulted in yellow to orange points. The image in panel C was shown graphically as a pixel fluorogram (panel D). The yellow/orange points along the diagonal of the fluorogram denote colocalized SCP_2 with catalase.

15 kDa pro-SCP-2 were postranslationally cleaved prior to entering the peroxisome, then the extraperoxisomally cleaved 13 kDa SCP-2 would not enter the peroxisome. The organelles staining with anti-SCP-2 antisera but not anti-catalase have been previously identified by immunofluorescence and immunogold microscopy as mitochondria and endoplasmic reticulum (*67*−*70*). Likewise, the nonpunctate, diffuse labeling has been identified as cytosolic (*68*, *71*, *72*). In summary, the C-terminal SKL peroxisomal targeting sequence alone was not sufficient for targeting SCP-2 to peroxisomes. Instead, peroxisomal targeting also required the 20 amino acid N-terminal presequence of the 15 kDa pro-SCP-2. That the C-terminal SKL of 15 kDa pro-SCP-2 is also required for peroxisomal targeting is shown by the lack of peroxisomal targeting of 15 kDa pro-SCP-2 from which the C-terminal amino acid had been removed by carboxypeptidase (*73*).

Indirect Immunofluorescence Confocal Imaging of SCP-2 Colocalization with Lysosomes. The above experiments were repeated to determine if the extraperoxisomal staining of cells transfected with the cDNA encoding for 15 kDa pro-SCP-2 was present not only as diffuse cytoplasmic staining, but also localized in part to lysosomes. The transfected L-cells were fixed and simultaneously labeled for SCP-2 with Texas Red-conjugated secondary antibody (Figure 11A) and for lysosomal membrane LAMP2 with FITC-conjugated antibody (Figure 11B). The laser scanning confocal microscopic fluorescence image showed that the pattern of anti-SCP-2 staining was largely punctate, with small size dots (Figure 11B). In contrast, staining of lysosomes with anti-LAMP2 showed a punctate pattern, but with heterogeneous sized dots (Figure 11B). Merging of these two simultaneously acquired confocal images (Figure 11C) showed substantial separate anti-SCP-2 (red) and anti-LAMP2 (green) staining. There was, however, little colocalization (yellow areas) of the two proteins (Figure 11C), confirmed by the pixel scattergram (Figure 11D) which showed only a small area of yellow pixels around the diagonal. Western blots of isolated lysosomes confirmed that the lysosomal membranes contained almost no SCP-2 (data not shown). These data suggested that SCP-2 was not significantly bound to or located within lysosomes.

DISCUSSION

The majority of cholesterol and cholesterol ester enters the cell via the LDL-receptor-mediated lysosomal pathway

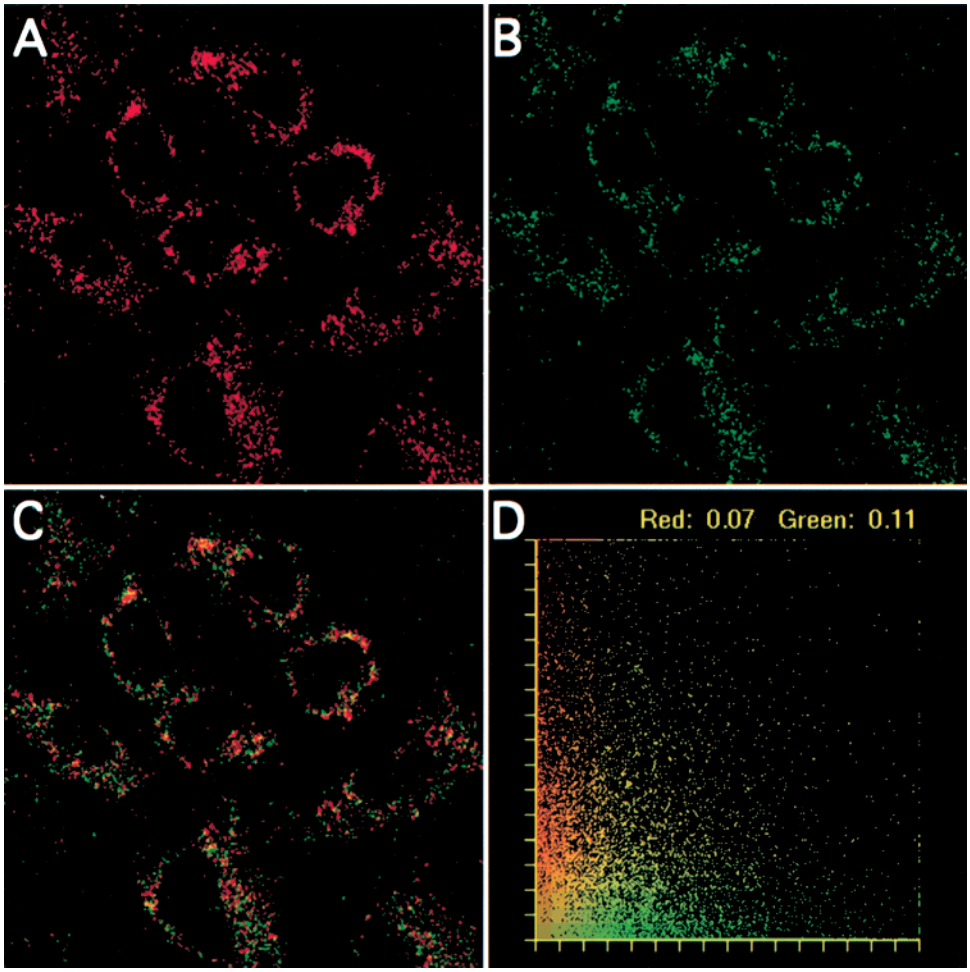

FIGURE 10: Confocal immunofluorescence imaging of L-cell fibroblasts transfected with the cDNA encoding 13 kDa SCP-2: colocalization of SCP-2 with peroxisomal catalase. L-cells overexpressing 13 kDa SCP_2 were simultaneously labeled with rabbit anti-SCP_2 and sheep anti-catalase followed by a Texas Red-conjugated IgG anti-rabbit secondary antibody (A, C) and FITC-conjugated IgG anti-sheep secondary antibody (B, C). Simultaneous double-label confocal images were acquired with a MRC 1024 laser scanning confocal microscopy system (Bio-Rad) with 63× objective and Axiovert 135 microscope (Zeiss Inc.). Images are shown for SCP_2 (red, panel A) and catalase (green, panel B). Superposition of panels A and B yielded a merged image (panel C). Colocalized SCP_2 (red) with catalase (green) resulted in yellow to orange points. The image in panel C was shown graphically as a pixel fluorogram (panel D). The yellow/orange points along the diagonal of the fluorogram denote colocalized SCP_2 with catalase.

(*74*). However, almost nothing is known regarding how cholesterol leaves the lysosomal matrix, enters the lysosomal membrane, translocates to the cytofacial leaflet, and transfers from the lysosomal membrane to the cytoplasm. Prior to the work presented herein, to our knowledge, there have been no reports characterizing the lysosomal membrane in terms of either cholesterol content or dynamics. The present investigation makes several new contributions offering insights into lysosomal membrane cholesterol dynamics and transfer of cholesterol out of the lysosome.

First, the lipid content of the purified lysosomal membrane, especially cholesterol, was unique, being intermediate between that of the plasma membrane and subcellular organelle membranes. To our knowledge, prior to the present investigation, there have been no previous reports examining the lipid composition of the isolated lysosomal membrane. Although the lipid composition of whole lysosomes isolated after Triton or dextran treatment of animals has been reported (*13*−*15*), these isolated organelles are known to contain other lipids besides those of the lysosomal membrane, e.g., lipoprotein lipids (*12*). As shown in the present investigation, L-cell lysosomal membranes exhibited a phospholipid:protein ratio, 320 μg/mg of protein, very similar to that of other subcellular membranes including plasma membranes, microsomes, and mitochondria (*30*). In contrast, the cholesterol:protein ratio of the L-cell lysosomal membranes (46 μg/mg of protein) differed markedly from other intracellular membranes in the following order: plasma membrane > lysosomal membrane > microsomal membrane ≫ mitochondrial membrane. The lysosomal membrane cholesterol:phospholipid ratio (0.38 mol/mol) was intermediate between plasma membranes and other intracellular organelles: the mean value for plasma membranes taken from seven different publications, 0.65 ± 0.07; endoplasmic reticulum, 0.16−0.23; mitochondria, 0.03 (reviewed in ref *75*). Finally, the lysosomal membrane cholesterol:phospholipid ratio was maintained constant regardless of whether the cells were cultured with cholesterol-containing medium (10% fetal bovine serum), cultured with cholesterol-free medium (serum-deficient medium) for 16 h, or cultured with 10% fetal bovine serum to which 0−40 μg of dehydroergosterol/mL had been added. This indicated that (i) the sterol content of the lysosomal membrane was closely regulated despite a large flux of sterol through the lysosome, and (ii) dehydroergosterol replaced cholesterol without adversely altering the lysosomal membrane sterol content. The finding that dehy-

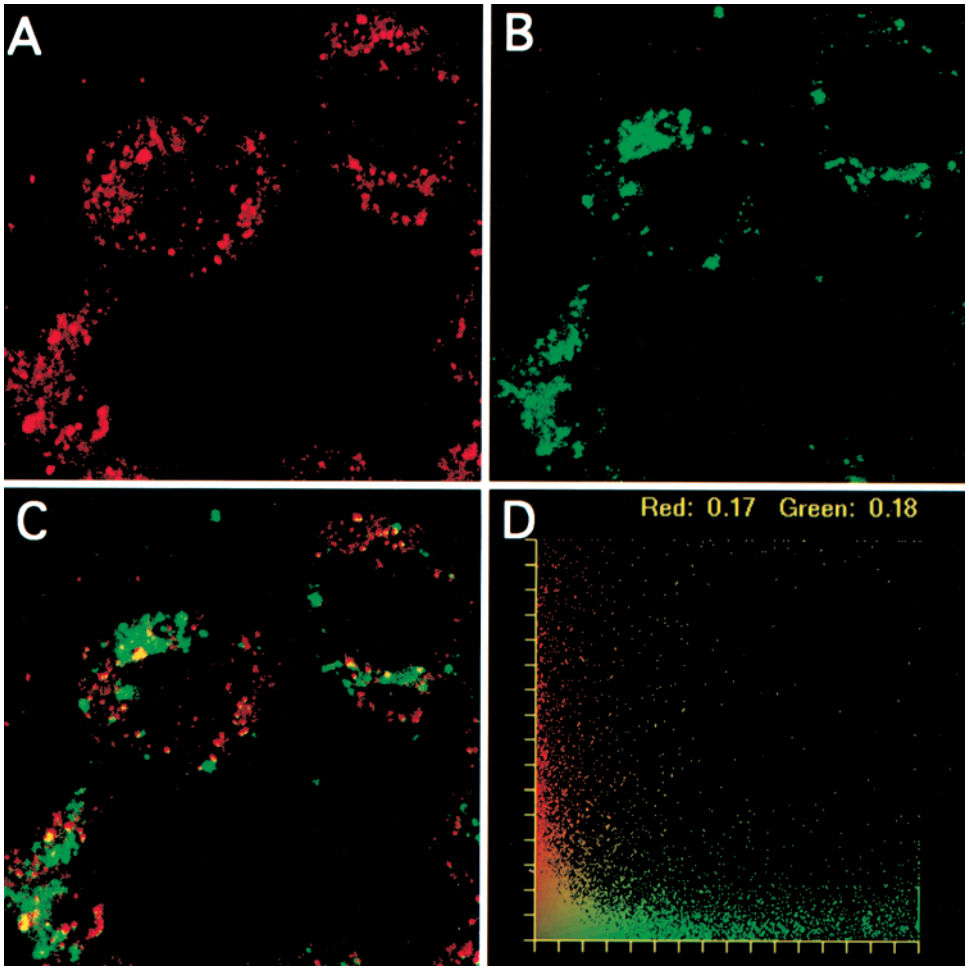

FIGURE 11: Confocal immunofluorescence imaging of SCP-2 and lysosomal LAMP2 in transfected L-cell fibroblasts overexpressing 15 kDa pro-SCP-2. Cells were simultaneously labeled with anti-SCP-2 and anti-LAMP2 followed by a Texas Red-conjugated secondary antibody to anti-SCP-2 (A, C) and FITC-conjugated secondary antibody to anti-LAMP2 (B, C). Simultaneous double-label confocal images were acquired with a MRC 1024 laser scanning confocal microscopy system (Bio-Rad) with 63× objective and Axiovert 135 microscope (Zeiss Inc.). Images are shown for anti-SCP-2 (red, panel A) and anti-LAMP2 (green, panel B). Superposition of panels A and B yielded a merged image (panel C). Colocalized SCP-2 (red) with LAMP2 (green) resulted in yellow to orange points. The image in panel C was shown graphically as a pixel fluorogram (panel D). The yellow/orange points along the diagonal of the fluorogram denote colocalized SCP-2 with LAMP2.

droergosterol codistributed with cholesterol in lysosomal membranes was consistent with earlier findings demonstrating codistribution of dehydroergosterol with cholesterol in plasma membranes, microsomes, and mitochondria isolated from L-cells (*25*). Dehydroergosterol codistribution with cholesterol in intact cells was recently confirmed by fluorescence microscopy (*48, 76*) and laser scanning multiphoton excitation microscopy (*48*).

Second, based on the rapid (2 min) transfer of cholesterol from the lysosome to the plasma membrane of intact cells (*10*), it was previously concluded that sterol spontaneously transferred out of the lysosome via lysosomal membrane primarily by fast passive diffusion (*11*). However, prior to the results presented herein, direct data testing this possibility were not available. The present results directly demonstrated the dynamics of sterol transfer from the isolated lysosome and from the purified lysosomal membrane. Surprisingly, it was found that spontaneous transfer of sterol out of the lysosome and out of the lysosomal membrane was extremely slow (initial rate of 0.010 ± 0.002 pmol/min, Table 1). When compared under identical assay conditions to other organelles isolated from L-cells, this initial rate for sterol egress from the lysosomal membrane was 63-fold, 41-fold, and 60-fold slower than from plasma membranes, microsomes, or mitochondria, respectively (*39*). Taken together with the reported half-time of LDL cholesterol ester-derived cholesterol leaving the lysosome in intact cells of 2 min (*10*), this indicates that spontaneous diffusional transfer of cholesterol from the lysosomal membrane to the cytoplasm does account for the rapid trafficking of LDL cholesterol (unesterified and cholesterol ester-derived) out of the lysosome. Likewise, although there is some evidence for the involvement of lysosomal membrane protein(s) in transfer of cholesterol out of the lysosome (*77*−*79*), the fact that spontaneous sterol transfer out of purified lysosomes as well as lysosomal membranes was extremely slow suggests that putative cholesterol transport protein(s) intrinsic to the lysosomal membrane is(are) alone not sufficient to account for the rapid transfer of cholesterol from lysosomes in intact cells.

Third, the lysosomal membrane cholesterol had a unique kinetic distribution into a single, very slowly or essentially nonexchangeable sterol pool/domain with half-time of exchange >4 days. This lysosomal membrane cholesterol organization differed significantly from that of all other mammalian membranes heretofore tested. All other subcellular membranes previously reported have at least some

exchangeable cholesterol pool/domain: 15−20% for human erythrocyte plasma membrane (*16*, *80*, *81*), 15% for fibroblast mitochondrial membranes (*39*), 40−60% for fibroblast plasma membranes and microsomal membranes (*39*), 27−50% for synaptosomal plasma membranes (*82*). In addition, all other previously examined subcellular membranes were much less susceptible to the action of SCP-2, which stimulated sterol transfer or induced formation of a rapidly exchangeable domain in the following relative order: lysosomal membrane (60−80-fold) ≫ plasma membrane (6-fold) > microsomal membrane and mitochondrial membrane (2-fold) ≫ erythrocyte plasma membrane (no stimulation). These differences were not due simply to the cholesterol content of the respective membranes since the cholesterol content of lysosomal membranes was intermediate between that of microsomal membranes and plasma membranes. In summary, the lysosomal membrane presented a unique kinetic organization of cholesterol. Probing with sterol-binding proteins such as SCP-2 enhanced sterol transfer from the lysosomal membrane up to 80-fold and specifically induced formation of a rapidly exchangeable domain of cholesterol.

Intermembrane cholesterol transfer has been postulated to occur by at least three potential mechanisms: spontaneous, vesicular, and protein carrier mediated. As shown above, the very slow spontaneous rate of sterol transfer out of the isolated lysosome and lysosomal membrane (days), as compared to that measured in intact cells (2 min) (*10*), was inconsistent with a spontaneous diffusion mechanism accounting for a significant part of cholesterol egress from the lysosome and lysosomal membrane.

While vesicular cholesterol transfer/shedding out of the lysosome was originally not thought to be a major mechanism for rapid cholesterol exit from the lysosome (reviewed in ref *12*), the recent discovery that the Niemann−Pick C1 (NPC1) protein is a transmembrane protein with a sterol-sensing domain has shed new light on the possibility that cholesterol may also exit the lysosome by vesicular transfer (*78*). In Niemann−Pick C1 disease, a mutant NPC1 protein inhibits cholesterol trafficking out of the lysosome and results in lysosomal and Golgi accumulation of cholesterol (*83*). The NPC1 protein is extensively colocalized with LAMP2, a marker for both lysosomes and late endosomes (*79*). Furthermore, within the latter population the NPC1 protein is distributed to a unique, late endosomal compartment distinct from LDL cholesterol laden lysosomes or endosomes containing adaptins, cathepsin, or mannose 6-phosphate receptor (*79*). The turnover time of the NPC1 vesicular compartment (1 h in normal cells) was nearly 2-fold slower in NPC1 disease, but the turnover rate of the lysosomal compartment was unchanged (*79*). Taken together, these data suggest that transport of cholesterol out of this unique, NPC1-containing vesicular pool was defective in NPC1 disease. Interestingly, it was pointed out that the NPC1 vesicles have certain characteristics resembling those of caveolar vesicles. Caveolar vesicles are thought to be involved in cholesterol trafficking between Golgi/endoplasmic reticulum and the plasma membrane (*4*). Furthermore, caveolin is upregulated in both murine and human NPC1 disease (*84*−*86*). Whether the increased caveolin expression represents a compensatory mechanism for the slow lysosomal cholesterol egress via NPC1 vesicles or both NPC1 and caveolin are present in the same endocytic compartment is not yet clear. Whether the 2-fold effect of NPC1 on cholesterol egress out of the NPC1 vesicular pool (*79*) alone is sufficient to account for the large accumulation of cholesterol in NPC1 disease is as yet unclear. Certainly the maximal stimulation of cholesterol transfer by SCP-2 was up to 40-fold greater than that by NPC1. The range of SCP-2 concentrations (<0.1−2.5 μM) used herein was close to the physiological range as found in high expression tissues (<0.08% of soluble protein or about <20 μM in liver, intestine, and steroidogenic tissues) and low expression tissues (<0.008% of soluble protein or <2 μM in brain etc.) (reviewed in ref *87*). Furthermore, SCP-2 induced formation of a rapidly exchangeable sterol domain in lysosomal membranes. The half-time for exchange of this domain, near 5 min, was remarkably similar to that observed for cholesterol transfer out of the lysosome to the plasma membrane in intact cells, i.e., 2 min (*10*). In contrast, the turnover time of cholesterol in the NPC1 vesicular compartment (1 h) is much longer than that of the rapidly exchangeable sterol domain induced by SCP-2 (5 min) or that reported for lysosomal cholesterol egress and transfer to the plasma membrane in intact cells (2 min) (*10*). Interestingly, SCP-2 is down-regulated by 70−90% in NPC1 disease (*88*). In short, exciting recent data showing a 2-fold slower egress rate of cholesterol from a unique, NPC1-containing, late endosomal vesicle pool are consistent with the possibility that cholesterol may exit the lysosome at least in part by vesicular transfer.

The last mechanism considered is the protein carrier mechanism for lysosomal cholesterol egress. At least two potential protein candidates that form soluble complexes with cholesterol have been identified, caveolin (*4*, *89*) and SCP-2 (*47*−*49*, *90*). Furthermore, as shown herein and earlier (reviewed in ref *48*) for SCP-2 as well as elsewhere for caveolin (*4*), both proteins enhance cholesterol transfer between membranes in vitro or in intact cells.

While the fact that SCP-2 [present work and (*68*)] and also caveolin (*4*) do not colocalize significantly with lysosomes suggests that neither protein may be the actual molecule directly enhancing cholesterol efflux out of the lysosome (*91*), a direct interaction of these proteins with the lysosomal membrane may not be required to enhance cholesterol transfer. Alternate possibilities include the following: (i) Increasing the aqueous solubility of cholesterol. Since the critical micellar concentration of cholesterol is extremely low, near 20 nM, very little cholesterol is able to freely diffuse between membranes. By binding cholesterol, SCP-2 or caveolin increase the aqueous partition of cholesterol away from membranes and may thereby enhance intermembrane sterol transfer. As shown herein and elsewhere (*89*), significant portions of SCP-2 and caveolin are present in the cytosol not bound to membranes and can consequently increase the aqueous solubility of cholesterol. Such a mechanism not requiring direct interaction of a lipid transfer protein with membranes has been demonstrated for liver fatty acid binding protein mediated transfer of fatty acids between membranes (reviewed in refs *92*−*94*). (ii) These proteins may act indirectly by interacting with the vesicular transfer pathway. Caveolin clearly also associates with caveolar vesicles (*4*). Whether SCP-2 similarly associates with cholesterol transfer vesicles or possibly enhances vesicular trafficking through its ability to bind polyphos-

phoinositides (*46*) or ligands (fatty acids or fatty acyl CoAs) that interact with nuclear regulatory proteins (PPAR or HNF4α) remains to be determined. Regardless of which mechanism(s) may be involved, with some exception (*61*, *91*) most of the available evidence suggests that SCP-2 participates in mediating cholesterol transfer within the cell (reviewed in refs *45*, *48*, *95*).

In summary, the data presented herein for the first time characterized the lysosomal membrane cholesterol and its cholesterol dynamics. The lysosomal membrane was unique in its cholesterol:phospholipid ratio being intermediate between the plasma membrane and other subcellular organelles. Significantly, spontaneous sterol transfer from lysosomes and from purified lysosomal membranes was extremely slow, half-time >4days, and up to 63-fold slower as compared to other cellular membranes. The observation of extremely slow (almost negligible) spontaneous sterol transfer from lysosomal membranes coupled with rapid (2 min) transfer in intact cells suggested that other factors extrinsic to the lysosome must be involved in mediating cholesterol transfer from the lysosomal membranes. The data were consistent with a protein-mediated mechanism(s) for lysosomal lipid efflux that exhibits substrate specificity (*77*) and may involve vesicular transport (NPC1 vesicles and caveolar vesicles) as well as aqueous protein-mediated transport (caveolin/chaperonin/cholesterol complexes, SCP-2, or as yet unidentified proteins). While the relative contributions of these mechanisms to lysosomal cholesterol egress are not yet entirely clear, the data presented herein suggest that proteins intrinsic to the lysosomal membrane are not alone sufficient for mediating rapid sterol transfer out of the lysosome and lysosomal membrane. That vesicular and protein-mediated intracellular cholesterol trafficking are intimately linked is suggested by studies wherein fibroblasts treated with antisense cDNA to SCP-2 exhibited compensatory upregulation of vesicular cholesterol transport (*96*).

ACKNOWLEDGMENT

The helpful advice of Dr. L. Liscum in purifying liposomes was much appreciated.

REFERENCES

1. Goldstein, J. L., and Brown, M. S. (1992) *Eur. J. Biochem. 13*, 34−36.
2. Fielding, C. J., Bist, A., and Fielding, P. E. (1998) in *Intracellular Cholesterol Trafficking* (Chang, T. Y., and Freeman, D. A., Eds.) pp 273−288, Kluwer Academic Publishers, Boston.
3. Krieger, M. (1999) *Annu. Rev. Biochem. 68*, 523−558.
4. Smart, E. J., and van der Westhuyzen, D. R. (1998) in *Intracellular Cholesterol Trafficking* (Chang, T. Y., and Freeman, D. A., Eds.) pp 253−272, Kluwer Academic Publishers, Boston.
5. Porpaczy, Z., Tomasek, J. J., and Freeman, D. A. (1997) *Exp. Cell Res. 234*, 217−224.
6. Hornick, C. A., Hui, D. Y., and DeLamatre, J. G. (1997) *Am. J. Physiol. 273*, C1075−C1081.
7. Fielding, C. J., and Fielding, P. E. (1997) *J. Lipid Res. 38*, 1503−1521.
8. Lange, Y., Ye, J., and Chin, J. (1997) *J. Biol. Chem. 272*, 17018−17022.
9. Johnson, W. J., Chacko, G. K., Phillips, M. C., and Rothblat, G. H. (1990) *J. Biol. Chem. 265*, 5546−5553.
10. Brasaemle, D. L., and Attie, A. D. (1990) *J. Lipid Res. 31*, 103−112.
11. Lloyd, J. B. (1996) in *Biology of the Lysosome* (Lloyd, J. B., and Mason, R. W., Eds.) pp 361−386, Plenum Press, New York.
12. Johnson, W. J., Warner, G. J., Yancey, P. G., and Rothblat, G. (1996) in *Biology of the Lysosome* (Lloyd, J. B., and Mason, R. W., Eds.) pp 239−293, Plenum Press, New York.
13. Matsuzawa, Y., and Hostetler, K. Y. (1980) *J. Biol. Chem. 255*, 646−652.
14. Colbeau, A., Nachbaur, J., and Vignais, P. M. (1971) *Biochim. Biophys. Acta 249*, 462−492.
15. Thines-Sempoux, D. (1973) in *Lysosomes in Biology and Pathology* (Dingle, J. T., Ed.) pp 278−299, North-Holland, Amsterdam.
16. Kavecansky, J., Joiner, C. H., and Schroeder, F. (1994) *Biochemistry 33*, 2880−2890.
17. Fischer, R. T., Stephenson, F. A., Shafiee, A., and Schroeder, F. (1984) *Chem. Phys. Lipids 36*, 1−14.
18. Fischer, R. T., Stephenson, F., Shafiee, A., and Schroeder, F. (1985) *J. Biol. Phys. 13*, 13−24.
19. Matsuura, J. E., George, H. J., Ramachandran, N., Alvarez, J. G., Strauss, J. F. I., and Billheimer, J. T. (1993) *Biochemistry 32*, 567−572.
20. Nemecz, G., Hubbell, T., Jefferson, J. R., Lowe, J. B., and Schroeder, F. (1991) *Arch. Biochem. Biophys. 286*, 300−309.
21. Nemecz, G., Jefferson, J. R., and Schroeder, F. (1991) *J. Biol. Chem. 266*, 17112−17123.
22. Atshaves, B. P., Petrescu, A., Starodub, O., Roths, J., Kier, A. B., and Schroeder, F. (1999) *J. Lipid Res. 40*, 610−622.
23. Moncecchi, D. M., Murphy, E. J., Prows, D. R., and Schroeder, F. (1996) *Biochim. Biophys. Acta 1302*, 110−116.
24. Frolov, A., Woodford, J. K., Murphy, E. J., Billheimer, J. T., and Schroeder, F. (1996) *J. Biol. Chem. 271*, 16075−16083.
25. Hale, J. E., and Schroeder, F. (1982) *Eur. J. Biochem. 122*, 649−661.
26. Storrie, B., and Madden, E. A. (1997) in *Methods in Enzymology*, pp 203−225, Academic Press, Inc., New York.
27. Madden, E. A., Wirt, J. B., and Storrie, B. (1987) *Arch. Biochem. Biophys. 257*, 27−38.
28. Ohsumi, Y., Ishizuka, T., and Kato, K. (1983) *J. Biochem. (Tokyo) 93*, 547−556.
29. Lowry, O. H., Rosebrough, N. J., Farr, A. L., and Randall, R. J. (1951) *J. Biol. Chem. 193*, 264−275.
30. Schroeder, F., Perlmutter, J. F., Glaser, M., and Vagelos, P. R. (1976) *J. Biol. Chem. 251*, 5015−5026.
31. Woodford, J. K., Hapala, I., Jefferson, J. R., Knittel, J. J., Kavecansky, J., Powell, D., Scallen, T. J., and Schroeder, F. (1994) *Biochim. Biophys. Acta 1189*, 52−60.
32. Incerpi, S., Jefferson, J. R., Wood, W. G., Ball, W. J., and Schroeder, F. (1992) *Arch. Biochem. Biophys. 298*, 35−42.
33. Pool, R. R., Maury, K. M., and Storrie, B. (1983) *Cell Biol. Int. Rep. 7*, 361−367.
34. Aronson, N. N., and Touster, O. (1985) *Methods Enzymol. 31*, 90.
35. Gossett, R. E., Edmondson, R. D., Jolly, C. A., Cho, T. H., Russell, D. H., Knudsen, J., Kier, A. B., and Schroeder, F. (1998) *Arch. Biochem. Biophys. 350*, 201−213.
36. Atshaves, B. P., Foxworth, W. B., Frolov, A. A., Roths, J. B., Kier, A. B., Oetama, B. K., Piedrahita, J. A., and Schroeder, F. (1998) *Am. J. Physiol. 274*, C633−C644.
37. Murphy, E. J., and Schroeder, F. (1997) *Biochim. Biophys. Acta 1345*, 283−292.
38. Hapala, I., Kavecansky, J., Butko, P., Scallen, T. J., Joiner, C., and Schroeder, F. (1994) *Biochemistry 33*, 7682−7690.
39. Frolov, A. A., Woodford, J. K., Murphy, E. J., Billheimer, J. T., and Schroeder, F. (1996) *J. Lipid Res. 37*, 1862−1874.
40. Butko, P., Hapala, I., Scallen, T. J., and Schroeder, F. (1990) *Biochemistry 29*, 4070−4077.
41. Butko, P., Hapala, I., Nemecz, G., and Schroeder, F. (1992) *J. Biochem. Biophys. Methods 24*, 15−37.

42. Nemecz, G., Fontaine, R. N., and Schroeder, F. (1988) *Biochim. Biophys. Acta 943*, 511−521.
43. Nemecz, G., and Schroeder, F. (1988) *Biochemistry 27*, 7740−7749.
44. Schroeder, F., Jefferson, J. R., Kier, A. B., Knittell, J., Scallen, T. J., Wood, W. G., and Hapala, I. (1991) *Proc. Soc. Exp. Biol. Med. 196*, 235−252.
45. Chanderbhan, R. F., Kharoubi, A., Pastuszyn, A., Gallo, L. L., and Scallen, T. (1998) in *Intracellular Cholesterol Trafficking* (Chang, T. Y., and Freeman, D. A., Eds.) pp 197−212, Kluwer Academic Publishers, Boston.
46. Gadella, T. W., Jr., and Wirtz, K. W. (1991) *Biochim. Biophys. Acta 1070*, 237−245.
47. Schroeder, F., Butko, P., Nemecz, G., and Scallen, T. J. (1990) *J. Biol. Chem. 265*, 151−157.
48. Schroeder, F., Frolov, A., Schoer, J., Gallegos, A., Atshaves, B. P., Stolowich, N. J., Scott, A. I., and Kier, A. B. (1998) in *Intracellular Cholesterol Trafficking* (Chang, T. Y., and Freeman, D. A., Eds.) pp 213−234, Kluwer Academic Publishers, Boston.
49. Stolowich, N. J., Frolov, A., Petrescu, A., Scott, A. I., Billheimer, J. T., and Schroeder, F. (1999) *J. Biol. Chem. 274*, 35425−35433.
50. Weber, G. (1954) *Trans. Faraday Soc. 50*, 552−555.
51. Smythe, E. (1996) in *Biology of the lysosome* (Lloyd, J. B., and Mason, R. W., Eds.) pp 51−92, Plenum Press, New York.
52. Schroeder, F., and Kinden, D. A. (1983) *J. Biochem. Biophys. Methods 8*, 15−27.
53. Kallen, C. B., Billheimer, J. T., Summers, S. A., Stayrook, S. E., Lewis, M., and Strauss, J. F. (1998) *J. Biol. Chem 273*, 26285−26288.
54. Woodford, J. K., Behnke, W. D., and Schroeder, F. (1995) *Mol. Cell. Biochem. 152*, 51−62.
55. Woodford, J. K., Colles, S. M., Myers-Payne, S., Billheimer, J. T., and Schroeder, F. (1995) *Chem. Phys. Lipids 76*, 73−84.
56. Gadella, T. W., and Wirtz, K. W. (1994) *Eur. J. Biochem. 220*, 1019−1028.
57. Billheimer, J. T., and Gaylor, J. L. (1990) *Biochim. Biophys. Acta 1046*, 136−143.
58. Huang, H., Ball, J. A., Billheimer, J. T., and Schroeder, F. (1999) *Biochem. J. 344*, 593−603.
59. Huang, H., Ball, J. A., Billheimer, J. T., and Schroeder, F. (1999) *Biochemistry 38*, 13231−13243.
60. Fischer, R. T., Cowlen, M. S., Dempsey, M. E., and Schroeder, F. (1985) *Biochemistry 24*, 3322−3331.
61. Seedorf, U., Raabe, M., Ellinghaus, P., Kannenberg, F., Fobker, M., Engel, T., Denis, S., Wouters, F., Wirtz, K. W. A., Wanders, R. J. A., Maeda, N., and Assmann, G. (1998) *Genes Dev. 12*, 1189−1201.
62. Sams, G. H., Hargis, B. M., and Hargis, P. S. (1991) *Compar. Biochem. Phys. 99B*, 213−219.
63. Rolf, B., Oudenampsen-Kruger, E., Borchers, T., Faergeman, N. J., Knudsen, J., Lezius, A., and Spener, F. (1995) *Biochim. Biophys. Acta 1259*, 245−253.
64. Rustow, B., Hodi, J., Kunze, D., Reichmann, G., and Egger, E. (1978) *FEBS Lett. 95*, 225−228.
65. Jefferson, J. R., Slotte, J. P., Nemecz, G., Pastuszyn, A., Scallen, T. J., and Schroeder, F. (1991) *J. Biol. Chem. 266*, 5486−5496.
66. Wirtz, K. W. A. (1997) *Biochem. J. 324*, 353−360.
67. Gallegos, A., Schoer, J., Starodub, O., Kier, A. B., Billheimer, J. T., and Schroeder, F. (2000) *Chem. Phys. Lipids 105*, 9−29.
68. Keller, G. A., Scallen, T. J., Clarke, D., Maher, P. A., Krisans, S. K., and Singer, S. J. (1989) *J. Cell Biol. 108*, 1353−1361.
69. Mendis-Handagama, S. M., Watkins, P. A., Gelber, S. J., and Scallen, T. J. (1992) *Endocrinology 131*, 2839−2845.
70. Reinhart, M. P., Avart, S. J., Dobson, T. O., and Foglia, T. A. (1993) *Biochem. J. 295*, 787−792.
71. Ossendorp, B. C., Voorhout, W. F., Van Amerongen, A., Brunink, F., Batenburg, J. J., and Wirtz, K. W. A. (1996) *Arch. Biochem. Biophys. 334*, 251−260.
72. Van der Krift, T. P., Leunissen, J., Teerlink, T., van Heusden, G. P. H., Verklij, A. J., and Wirtz, K. W. A. (1985) *Biochim. Biophys. Acta 812*, 387−392.
73. Wouters, F., Bastiaens, P. I., Wirtz, K. W., and Jovin, T. M. (1998) *EMBO J. 17*, 7179−7189.
74. Brown, M. S., and Goldstein, J. L. (1986) *Science 232*, 34−47.
75. Schroeder, F., Frolov, A. A., Murphy, E. J., Atshaves, B. P., Jefferson, J. R., Pu, L., Wood, W. G., Foxworth, W. B., and Kier, A. B. (1996) *Proc. Soc. Exp. Biol. Med. 213*, 150−177.
76. Mukherjee, S., Zha, X., Tabas, I., and Maxfield, F. R. (1998) *Biophys. J. 75*, 1915−1925.
77. Sato, Y., Nishikawa, K., Aikawa, K., Mimura, K., Murakami-Murofushi, K., Arai, H., and Inoue, K. (1995) *Biochim. Biophys. Acta 1257*, 38−46.
78. Carstea, E. D., Morris, J. A., Coleman, K. G., Loftus, S. K., Zhang, D., Cummings, C., Gu, J., Rosenfeld, M. A., Pavan, W. J., Krizman, D. B., Nagle, J., Polymeropoulos, M. H., Sturley, S. L., Ioannou, Y. A., Higgins, M. E., Comly, M., Cooney, A., Brown, A., Kaneski, C. R., Blanchette-Mackie, E. J., Dwyer, N. K., Neufeld, E. B., Chang, T. Y., Liscum, L., Strauss, J. F., III, Ohno, K., Zeigler, M., Carmi, R., Sokol, J., Markie, D., O'Neill, R. R., van Diggelen, O. P., Elleder, M., Patterson, M. C., Brady, R. O., Vanier, M. T., Pentchev, P. G., and Tagle, D. A. (1997) *Science 277*, 228−231.
79. Neufeld, E. B., Wastney, M., Patel, S., Suresh, S., Cooney, A. M., Dwyer, N. K., Roff, C. F., Ohno, K., Morris, J. A., Carstea, E. D., Incardona, J. P., Strauss, J. F., Vanier, M. T., Patterson, M. C., Brady, R. O., Pentchev, P. G., and Blanchette-Mackie, E. J. (1999) *J. Biol. Chem. 274*, 9627−9635.
80. Kavecansky, J., Schroeder, F., and Joiner, C. H. (1995) *Am. J. Physiol. 269*, C1105−C1111.
81. Schroeder, F., Woodford, J. K., Kavecansky, J., Wood, W. G., and Joiner, C. (1995) *Mol. Membr. Biol. 12*, 113−119.
82. Rao, A. M., Igbavboa, U., Semotuk, M., Schroeder, F., and Wood, W. G. (1993) *Neurochem. Int. 23*, 45−52.
83. Pentchev, P. G., Brady, R. O., Blanchette-Mackie, E. J., Vanier, M. T., Carstea, E. D., Parker, C. C., Goldin, E., and Roff, C. F. (1994) *Biochim. Biophys. Acta 1225*, 235−243.
84. Garver, W. S., Hsu, S. C., Erickson, R. P., Greer, W. L., Byers, D. M., and Heidenreich, R. A. (1997) *Biochem. Biophys. Res. Commun. 236*, 189−193.
85. Garver, W. S., Hossain, G. S., Winscott, M. M., and Heidenreich, R. A. (1999) *Biochim. Biophys. Acta 1453*, 193−206.
86. Garver, W. S., Erickson, R. P., Wilson, J. M., Colton, T. L., Hossain, G. S., Kozloski, M. A., and Heidenreich, R. A. (1997) *Biochim. Biophys. Acta 1361*, 272−280.
87. Gossett, R. E., Frolov, A. A., Roths, J. B., Behnke, W. D., Kier, A. B., and Schroeder, F. (1996) *Lipids 31*, 895−918.
88. Roff, C. F., Pastuszyn, A., Strauss, J. F. I., Billheimer, J. T., Vanier, M. T., Brady, R. O., Scallen, T. J., and Pentchev, P. G. (1992) *J. Biol. Chem. 267*, 15902−15908.
89. Uittenbogaard, A., Ying, Y. S., and Smart, E. J. (1998) *J. Biol. Chem. 273*, 6525−6532.
90. Colles, S. M., Woodford, J. K., Moncecchi, D., Myers-Payne, S. C., McLean, L. R., Billheimer, J. T., and Schroeder, F. (1995) *Lipids 30*, 795−804.
91. Johnson, W. J., and Reinhart, M. P. (1994) *J. Lipid Res. 35*, 563−573.
92. Weisiger, R. A. (1996) *Comput. Biochem. Physiol. 115B*, 319−331.
93. Weisiger, R. A. (1998) *Hepatology 24*, 1288−1295.
94. McArthur, M. J., Atshaves, B. P., Frolov, A., Foxworth, W. D., Kier, A. B., and Schroeder, F. (1999) *J. Lipid Res. 40*, 1371−1383.
95. Leonard, A. N., and Cohen, D. E. (1998) *J. Lipid Res. 39*, 1981−1988.
96. Puglielli, L., Rigotti, A., Greco, A. V., Santos, M. J., and Nervi, F. (1995) *J. Biol. Chem. 270*, 18723−18726.

BI992686H